Palaeogeography, Palaeoclimatology, Palaeoecology 278 (2009) 24–39

Contents lists available at ScienceDirect

Palaeogeography, Palaeoclimatology, Palaeoecology

journal homepage: www.elsevier.com/locate/palaeo

The Messinian Salinity Crisis in the Dardanelles region: Chronostratigraphic constraints

Mihaela Carmen Melinte-Dobrinescu [a], Jean-Pierre Suc [b,*], Georges Clauzon [c], Speranta-Maria Popescu [b], Rolando Armijo [d], Bertrand Meyer [e], Demet Biltekin [f], M. Namık Çağatay [f], Gülsen Ucarkus [f], Gwénaël Jouannic [e], Séverine Fauquette [g], Ziyadin Çakir [f]

[a] National Institute of Marine Geology and Geo-ecology (GEOECOMAR), 23-25 Dimitrie Onciul Street, RO-024053 Bucharest, Romania
[b] Laboratoire PaléoEnvironnements et PaléobioSphère, UMR 5125, CNRS, France; Université Lyon 1, Campus de La Doua, Bâtiment Géode, 69622 Villeurbanne Cedex, France
[c] C.E.R.E.G.E. (UMR 6635 CNRS), Université Paul Cezanne, 13545 Aix-en-Provence Cedex, France
[d] Laboratoire de Tectonique, Institut de Physique du Globe de Paris (UMR 7154 CNRS), 75252 Paris Cedex, France
[e] Université Pierre et Marie Curie, ISTeP, UMR 7193, 75252 Paris Cedex 05, France
[f] Istanbul Technical University, School of Mines and Eurasia Institute of Earth Sciences, Maslak, 34469 Istanbul, Turkey
[g] Institut des Sciences de l'Evolution (UMR 5554 CNRS), Equipe Paléoenvironnements et Paléoclimats, CC 061, Université Montpellier 2, Place Eugène Bataillon, 34095 Montpellier Cedex 05, France

ARTICLE INFO

Article history:
Received 31 August 2008
Received in revised form 29 March 2009
Accepted 7 April 2009

Keywords:
Calcareous nannoplankton
Chronostratigraphy
Messinian Salinity Crisis
Palaeogeography
NE Aegean region

ABSTRACT

An intense controversy on chronostratigraphy of upper Miocene–lower Pliocene deposits and the Messinian Salinity Crisis in the Dardanelles area led to a systematic investigation of calcareous nannoplankton content of 10 key-sections representative of the most relevant regional Kirazlı and Alçıtepe formations. Our study shows clearly that the Kirazlı Formation deposits predate the Messinian Salinity Crisis while those of the Alçıtepe Formation postdate this outstanding event, which severely impacted the region as widely known around the Mediterranean Basin. Fluvial canyon cutting or gap in sedimentation linked to the peak of the Messinian Salinity Crisis separates the two formations. Detailed palaeoenvironmental investigations (based on the fluctuation and distribution pattern of dinoflagellate cysts, pollen grains and calcareous nannoplankton) allow us to reconstruct the regional palaeogeography before, during and after the Messinian Salinity Crisis. The gathered data do not indicate any marine corridor between the Eastern Mediterranean Sea and Eastern Paratethys through the Marmara Sea region at the time of the Messinian Salinity Crisis.

1. Introduction

During the Late Neogene, very significant paleobiogeographical changes have taken place in the Mediterranean region *s.l.*, fundamentally because the connection of the Atlantic Ocean with the Mediterranean Sea and the Paratethys (a residual continental sea which covered large areas of the Central and Eastern Europe) Sea was restricted and sometimes completely interrupted (Seneš, 1973; Rögl and Steininger, 1983; Marinescu, 1992; Mărunţeanu and Papaianopol, 1995; Rögl, 1998; Sprovieri et al., 2003; Clauzon et al., 2005; Popov et al., 2006; Popescu, 2006; Melinte, 2006). The latest Miocene is characterized by an exceptional event, which was the severe sea-level drop of the Mediterranean Sea, leading to the Messinian Salinity Crisis (MSC). This event is characterized throughout the Mediterranean basin by both, deposition of thick evaporites in its deep basins and cutting of huge fluvial canyons across its margins (Hsü et al., 1973; Clauzon, 1973; Cita et al., 1978; Clauzon et al., 1996). Such a prominent geological event produced significant changes in the palaeobiological assemblages, mirrored especially by the marine planktonic organisms (such as planktonic foraminifers, calcareous nannoplankton and dinoflagellates), which are very sensitive to environmental changes.

Consequently, the Messinian Salinity Crisis is now recognized as the most prominent event marking palaeobiogeographical change in the Mediterranean. Examples of case studies of spectacular features associated with the MSC are widespread over the entire Mediterranean area (for an overview, see: Agusti et al., 2006; Rouchy et al., 2006; Suc et al., 2007; CIESM, 2008). The present study is devoted to improving our knowledge of the MSC in the Dardanelles region (Fig. 1A), which is crucial for our understanding of the evolution of the linkage between the Aegean Sea and the Black Sea. The existence of a gateway at the time of the MSC is subject of controversy (in support of such a gateway, see: Esu, 2007; Faranda et al., 2007; Gliozzi et al., 2007; Stoica et al., 2007; in opposition of such a gateway, see: Clauzon et al., 2005;

* Corresponding author.
E-mail addresses: melinte@geoecomar.ro (M.C. Melinte-Dobrinescu), jean-pierre.suc@univ-lyon1.fr (J.-P. Suc), clauzon@cerege.fr (G. Clauzon), speranta.popescu@univ-lyon1.fr (S.-M. Popescu), armijo@ipgp.jussieu.fr (R. Armijo), bertrand.meyer@upmc.fr (B. Meyer), biltekin@itu.edu.tr (D. Biltekin), cagatay@itu.edu.tr (M.N. Çağatay), ucarkus1@itu.edu.tr (G. Ucarkus), gwenael.jouannic@gmail.com (G. Jouannic), severine.fauquette@univ-montp2.fr (S. Fauquette), ziyadin.cakir@itu.edu.tr (Z. Çakir).

0031-0182/$ – see front matter © 2009 Elsevier B.V. All rights reserved.
doi:10.1016/j.palaeo.2009.04.009

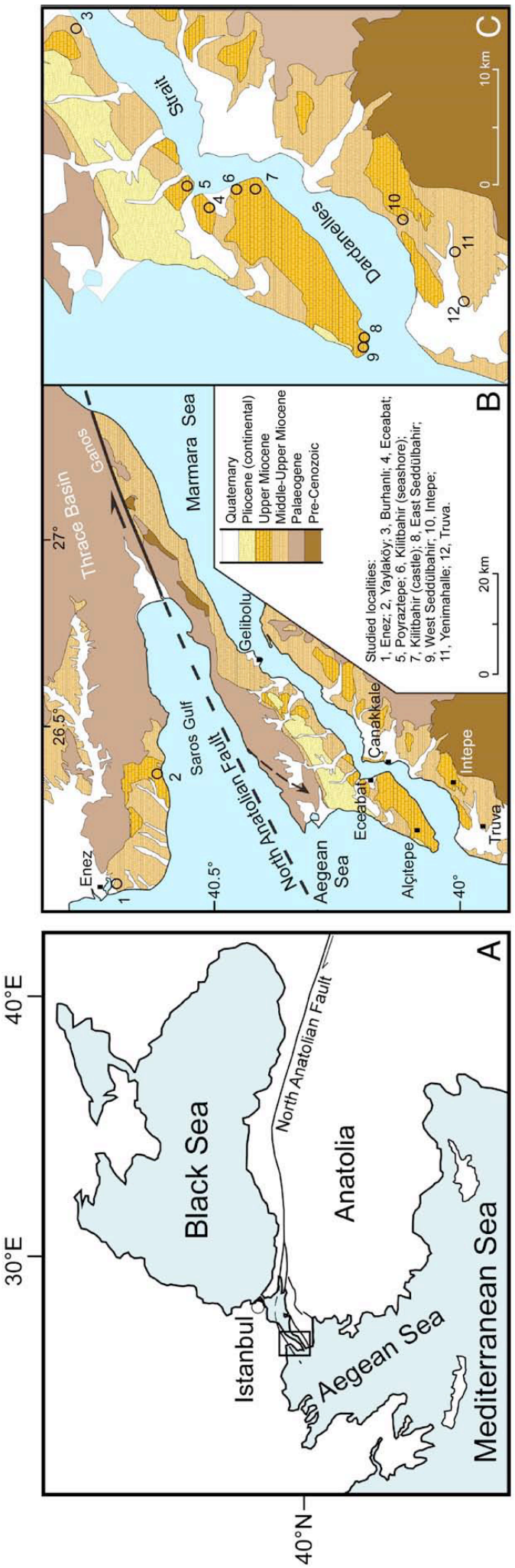

Fig. 1. Location and geological maps. A, Study area. B, Geological map of the studied area according to Türkecan and Yurtsever (2002). C, Geological map of the area surrounding the Dardanelles Strait according to Türkecan and Yurtsever (2002).

Popescu, 2006; Gillet et al., 2007; Popescu et al., 2009). However, most of the regional stratigraphic works underestimated the impact of the MSC in the Dardanelles (see, for examples: Görür et al., 1997; Çağatay et al., 1998; Görür et al., 2000; Türkecan and Yurtsever, 2002; Sakınç and Yaltırak, 2005; Çağatay et al., 2006). The consensus among regional stratigraphers is that the rocks outcropping in the Dardanelles are chiefly sediments of Eocene to Middle–Late Miocene Age and that the region is basically devoid of marine sediments of Pliocene Age (Fig. 1B, C). The typical strong marginal signature of the MSC is present all around the Mediterranean (including the Aegean Sea), with an erosional surface and deeply incised fluvial canyons, subsequently covered and filled with marine Pliocene sediments (examples from the Western Mediterranean: Clauzon, 1973, 1978, 1980a,b, 1982, 1990; Gautier et al., 1994; Clauzon, 1999; Guennoc et al., 2000; Lofi et al., 2003, 2005; Sage et al., 2005; Cornée et al., 2006; Maillard and Mauffret, 2006 — example from the Central Mediterranean: El Euch-El Koundi et al., 2009 — examples from the Eastern Mediterranean: Chumakov, 1973; Delrieu et al., 1993; Poisson et al., 2003). Even if these erosional effects of the MSC were suspected in the Dardanelles region (Çağatay et al., 2006), they were not clearly evidenced until today, mapped and recognized as such using conventional stratigraphy.

Defying the stratigraphical consensus, the study by Armijo et al. (1999) presented evidence for a widespread erosion surface and a prominent canyon that parallels the present-day Dardanelles Strait. These authors interpreted explicitly these features as possibly resulting from the MSC, given the large uncertainties in the ages of the formations mapped in the area (Ternek, 1964). Both the erosion surface and the canyon appear carved into the sediments of the Kirazlı Formation and filled by sediments of the Alçıtepe Formation (Armijo et al., 1999). Consequently, Armijo et al. (1999) deduced for these two formations a possible Messinian and an early Pliocene Age, respectively (Fig. 2). The study by Armijo et al. (1999) includes a geological map that shows strong folding affecting layers of the Kirazlı Formation, but not those of the overlying Alçıtepe Formation. Therefore, this important unconformity would also correlate roughly with the MSC, providing an invaluable constraint for the age of the propagation of the North Anatolian Fault across the region (Armijo et al., 1999). The work by Armijo et al. (1999) has been strongly criticized (e.g., Yaltırak et al., 2000 vs. Armijo et al., 2000) and its main stratigraphic inferences dismissed (e.g., Sakınç and Yaltırak, 2005; Çağatay et al., 2006).

In order to clarify the significance of the Messinian Salinity Crisis and its geological imprint in the Dardanelles region, we revised the stratigraphy by a systematic sampling of the most critical sedimentary units and by dating those using calcareous nannofossils. We studied ten key-sections (Enez and Yaylaköy in the Gulf of Saros; Burhanlı, Eceabat, Poyraztepe, Kilitbahir, Seddülbahir, Intepe, Yenimahalle and Truva in the Dardanelles Strait) where Upper Neogene deposits are well exposed (Fig. 1B, C). Our objectives are: (1) dating these sections with respect to global bio- chronostratigraphy using calcareous nannofossils, (2) reconstructing marine, brackish and continental palaeoenvironments using dinoflagellate cyst, calcareous nannoplankton and pollen grain fluctuations, and (3) setting up a reliable chronostratigraphic basis for current and future studies of the Messinian Salinity Crisis in the Dardanelles region, as well as for studies using the MSC as a chronometer for deformation associated with the North Anatolian Fault.

The age of the Alçıtepe Formation is the crucial question for the ongoing controversy (Fig. 2). The Alçıtepe Formation is described as being composed of brackish- to freshwater carbonates, interbedded with marine sandstones and siltstones (Görür et al., 1997; Çağatay et al.,

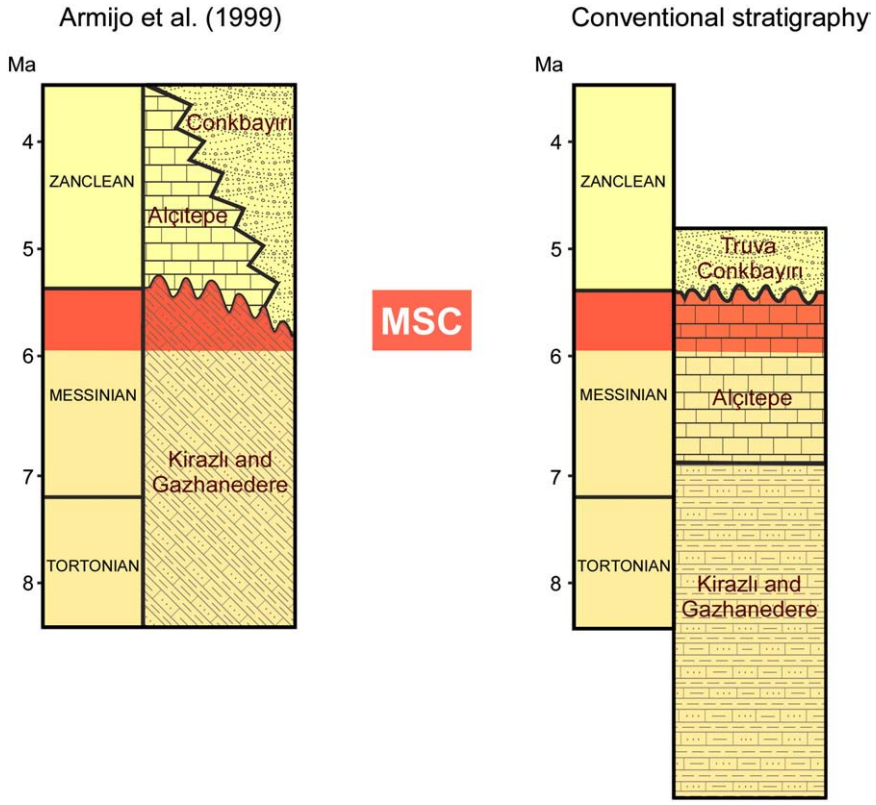

Fig. 2. Controversed age of the Neogene formations in the Dardanelles Strait area. Time-interval corresponding to the Messinian Salinity Crisis (MSC) is indicated by a red band. Defining the stratigraphic position of the Alçıtepe Formation with respect to the MSC is critical. The hypothesis represented to the left (Armijo et al., 1999) assigns a Pliocene Age (post-MSC) to the Alçıtepe Formation. The hypothesis that is currently proposed in the conventional stratigraphy (e.g., Görür et al., 1997; Sakınç et al., 1999; Türkecan and Yurtsever, 2002; Çağatay et al., 2006) assigns a Miocene Age (pre-MSC and partly coeval with it) to the Alçıtepe Formation. The undulating line represents an important erosion and tectonic unconformity in the hypothesis of Armijo et al. (1999), only a slight unconformity in the conventional stratigraphy. (For interpretation of the references to colour in this figure legend, the reader is referred to the web version of this article.)

1998) as more or less conformably overlying the Kirazlı Formation (Çağatay et al., 2006). It is overlain by shallow fluvio-marine siliciclastic rocks (Göztepe Formation in the North Marmara region, Truva Formation in the South Marmara region: Görür et al., 2000; Çağatay et al., 2006). A brackish Paratethyan fauna (i.e. *Mactra* sp., *Paradacna abichi*, *Dreissena* sp., *Cardium* sp., and *C. edulis*) was reported from the Alçıtepe Formation, suggesting that these deposits belong to the Pontian Paratethyan Stage (Gillet et al., 1978; Taner, 1979; Çağatay et al., 2006) and, as a consequence, to the so-called "late Messinian Lago Mare" (Sakınç and Yaltırak, 2005; Çağatay et al., 2006). Some intercalations of layers with Mediterranean marine faunas (*Ostrea*, *Pecten*) were also reported (Sakınç and Yaltırak, 2005), that emphasizes the dual, Paratethyan and Mediterranean, influence in the area. To characterize the MSC in the region, we focussed our study on the relationships between the Alçıtepe Formation and the underlying Kirazlı Formation.

2. Materials and methods

Calcareous nannoplankton investigations were performed for the sections Enez, Yaylaköy, Buhranlı, Eceabat, Poyraztepe, Kilitbahir, Seddülbahir, Intepe, Yenimahalle and Truva. To retain the original sample composition, smear slides were prepared directly from the untreated samples. The calcareous nannofloral analyses were performed using a light polarizing microscope at ×1600 magnification. The nannofloral taxonomic identification follows Perch-Nielsen (1985) and Young (1998).

Palynological samples were processed from some of these sections: Burhanlı (1 sample), Eceabat (1 sample), Seddülbahir (2 samples), and Intepe (10 samples). Each sample (20 g of dry sediment) was processed using standard method (Cour, 1974): acid digestion, concentration using $ZnCl_2$ (at density 2.0) and sieving at 10 µm. A 50 µl volume of residue was mounted between the coverslip and microscope slide using glycerine in order to allow rotation of palynomorphs for their complete examination resulting in their proper identification. Counting of palynomorphs was performed using a light microscope, their identification was done at ×1000 magnification. Pollen grains were identified with a botanical approach. 150 pollen grains except those of *Pinus* were identified and counted per sample. For the slides showing very poor concentrations in dinoflagellate cysts, a new sieving at 20 µm was performed on the pollen residue that permitted to concentrate the dinoflagellate cysts and a new slide was obtained using 50 µl from the new residue. Only the ten samples from the Intepe sections were analysed: all the specimens present on a slide were identified and counted. The freshwater algae *Pediastrum* and *Botryococcus* were considered as transported by rivers, and were also counted. Their vertical distribution documents duration and intensity of freshwater inputs.

3. Results

3.1. Bio- and chronostratigraphy

The calcareous nannoplankton offers an accurate way of biostratigraphic dating based on successive calibrated datum events within the time-window 8–4 Ma, which is of interest to this study. The calibration of the FAD (First Appearance Datum) and the LAD (Last Appearance Datum) follows Berggren et al. (1995), Backman and Raffi (1997), Lourens et al. (2004) and Raffi et al. (2003, 2006); we also took into account the available data for nannofloral distribution within the Messinian–Zanclean interval from the Eastern Mediterranean (i.e., Castradori, 1998; Snel et al., 2006; Wade and Bown, 2006). The distribution of six nannofossils was particularly useful for biostratigraphical purposes, as follows (Fig. 3): *Amaurolithus primus* (FAD: 7.424 Ma; LAD: 4.50 Ma; Plate I, Fig. 5), *Reticulofenestra rotaria* (FAD: ca. 7.41 Ma; LAD: imprecise, up to ca. 6 Ma; Plate I, Fig. 1), *Nicklithus* (= *Amaurolithus*) *amplificus* (FAD: 6.909 MA; LAD: 5.978 Ma; Plate I, Fig. 4), *Triquetrorhabdulus rugosus* (FAD: 12.671 Ma; LAD: 5.279 Ma; Plate I, Fig. 6), *Ceratolithus acutus* (FAD: 5.345 Ma; LAD: 5.040 Ma; Plate I, Figs. 2–3), and *Reticulofenestra pseudoumbilicus* (FAD: 8.761 Ma; LAD: 3.839 Ma). The absolute age of the FADs and LADs (after Raffi et al., 2003, 2006) is indicated as a rough guide; noticeably, when different ages are given for the same event, we accepted those proposing the largest range especially for the Eastern Mediterranean, when available. The nannofloral

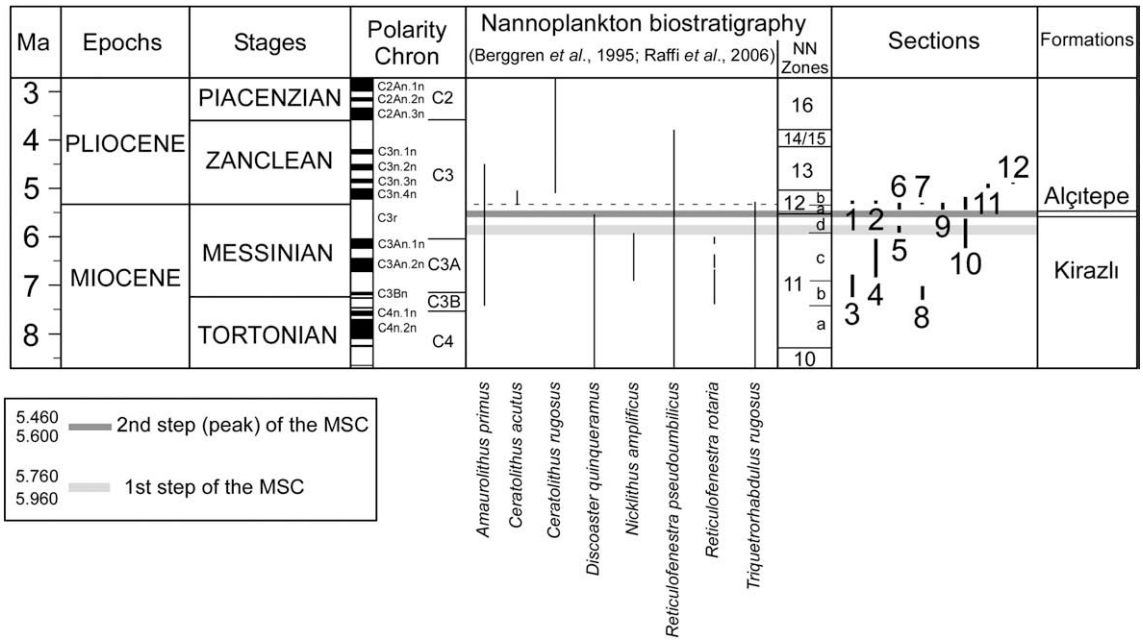

Fig. 3. Chronostratigraphy, calcareous nannoplankton biostratigraphy of the Late Miocene and Early Pliocene and inferred age of the studied sections. Chronology refers to Lourens et al. (2004), calcareous nannoplankton events according to Berggren et al. (1995) and Raffi et al. (2006). The grey strips correspond to two steps of the MSC (Clauzon et al., 1996) accepted by a representative community working on the Messinian Salinity Crisis (CIESM, 2008). Locality numbers, see Fig. 1B, C. The double line in the "Formations" column illustrates the lack of sedimentation during the peak of the MSC. It is to notice that the Yenimahalle and Truva sections are not located according to nannoplankton biostratigraphy but with respect to geomorphology and the reverse palaeomagnetism of the Yenimahalle section.

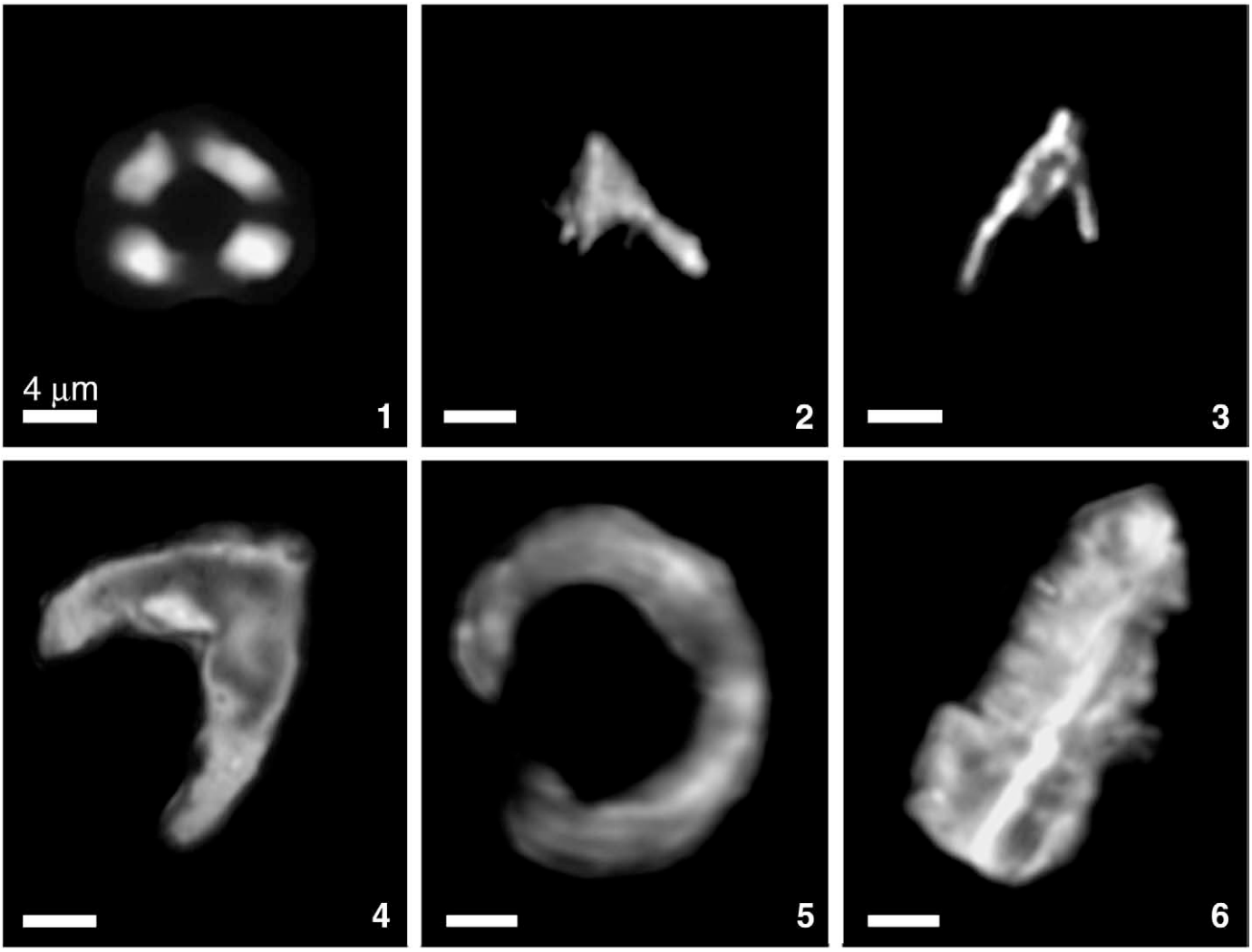

Plate I. Microphotographs of the significant biostratigraphic nannoplankton species (light microscope, crossed nicols, scale bar = 4 µm).

Fig. 1. *Reticulofenestra rotaria* Theodoridis; Eceabat (sample 1).
Fig. 2. *Ceratolithus acutus* Gartner and Bukry; Intepe (sample 24).
Fig. 3. *Ceratolithus acutus* Gartner and Bukry; Kilitbahir (sample 4).
Fig. 4. *Nicklithus amplificus* (Bukry and Percival) Gartner and Bukry; Intepe (sample 1).
Fig. 5. *Amaurolithus primus* (Bukry and Percival) Gartner and Bukry; Intepe (sample 35).
Fig. 6. *Triquetrorhabdulus rugosus* Bramlette and Wilcoxon; Kilitbahir (sample 4).

events (i.e., occurrence and extinction of the above-mentioned nannofossils) allow us to identify the NN11 and NN12 Zones of Martini (1971), including the subzones of Berggren et al. (1995). As done by Bukry (1975) and more recently used by Backman and Raffi (1997) for the global ocean, it appeared necessary to subdivide Zone NN12. We subdivided it into Subzones a and b, defined by the LAD of *Discoaster quinqueramus* and the FAD of *Ceratolithus acutus*, respectively. *D. quinqueramus* is rarely recorded in the Mediterranean, but its extinction occurred at the beginning of the peak of the MSC. The Messinian Erosional Surface may be considered as coeval of this bioevent, making the subdivision into Subzones NN12a and NN12b very useful in the Mediterranean region. Hence, the chronostratigraphic resolution in the Mediterranean can be improved in distinguishing post-Salinity Crisis sediments below the FAD of *C. acutus* from those above it (Fig. 3).

Concerning the nannofloral preservation observed in the studied samples, this is generally moderate, which means that dissolution and/or overgrowth of the nannofossils hindered the specific identification up to 25%. Some samples (i.e., from the lower part of the Intepe section) showed a good preservation; hence, the nannofloral specimens could be identified up to 90% to species level. A few samples (i.e., 14–21 from Intepe), contain nannofloral assemblages poorly preserved, showing severe dissolution, fragmentation and/or overgrowth; the specific identification being hindered up to 70%.

In general, the investigated samples contain nannofloral reworkings mainly from Cretaceous, Paleogene and Lower Miocene. The reworked taxa represent between 25 and 60% of the total recorded nannofloras. Hence, we may address questions about the possibility that some Miocene taxa, such as *Triquetrorhabdulus rugosus* and *Reticulofenestra pseudoumbilicus*, are *in situ* or reworked, impeding the accuracy of the biostratigraphical interpretation. *T. rugosus* is generally rare in the studied samples throughout its range (2–4 specimens/sample) and thus the possibility of this taxon being reworked into younger deposit is very low. *Reticulofenestra pseudoumbilicus* (>7 µm) is common in all the studies samples, being probably also common in the underlying Miocene deposits. But the fact that the recorded specimens of *R. pseudoumbilicus* are well-preserved, being found in assemblages yielding a moderate to good preservation, indicate that the nannofloral compositions are primary.

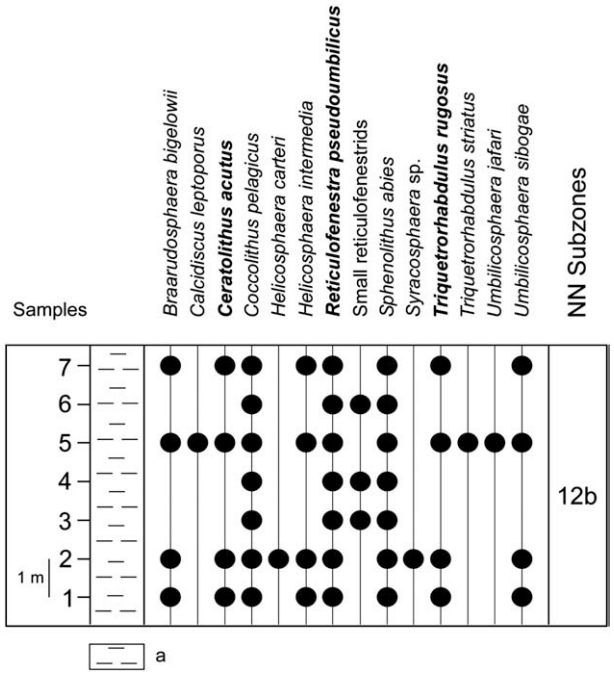

Fig. 4. Distribution and biostratigraphy of the calcareous nannofloras from the Enez locality. Nannoplankton biostratigraphic markers are in bold characters. a, Clay.

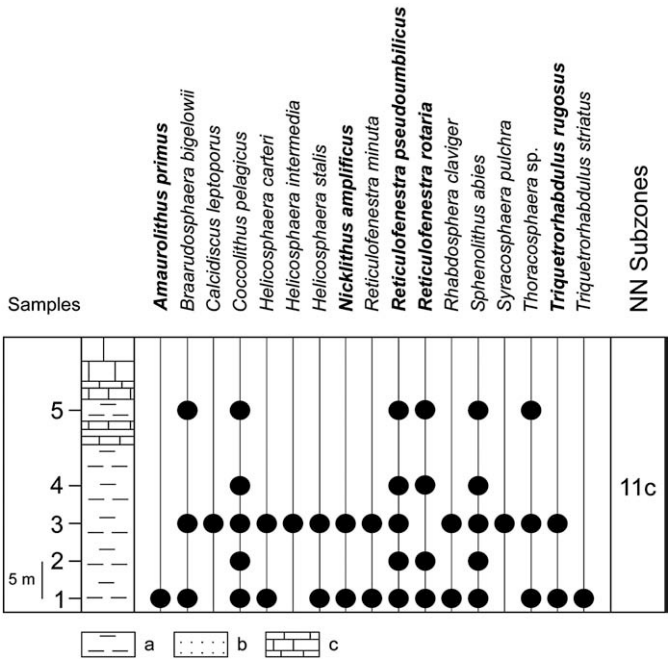

Fig. 6. Distribution and biostratigraphy of the calcareous nannofloras from the Eceabat locality. Nannoplankton biostratigraphic markers are in bold characters. a, Clay; b, Sand; c, Limestone.

3.1.1. Gulf of Saros

The studied section near Enez is located on the eastern shoreline of the Enez lagoon (40°46′24″ N latitude, 26°04′ E longitude; Fig. 1B), an area described as covered by deltaic deposits of the Meriç River overlying the Kirazlı Formation (Çağatay et al., 1998, 2006) while Sakınç et al. (1999) indicates some bioclastic carbonate rocks attributed to the Alçıtepe Fm., the upper part of which could belong to Zanclean. Here, brownish clays with a thickness of about 8 m have provided a poorly to moderately preserved nannoflora in 7 samples (Fig. 4). The co-occurrence of *Triquetrorhabdulus rugosus* and *Ceratolithus acutus* throughout the whole section is indicative for the NN12b nannofossil Subzone (Fig. 4), representing the extreme end of Messinian (after the MSC) to early Zanclean (Fig. 3).

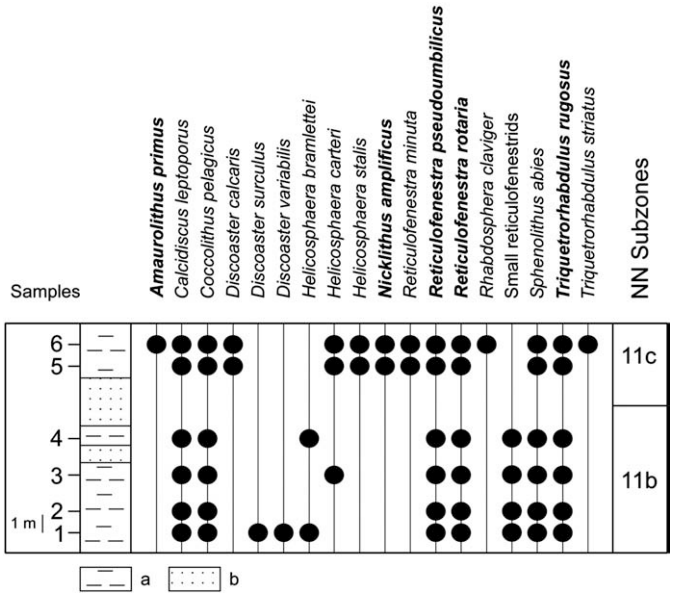

Fig. 5. Nannoflora of the Burhanlı locality with indication of nannoplankton subzones. Nannoplankton biostratigraphic markers are in bold characters. a, Clay; b, Sand.

At Yaylaköy, blue clays are exposed along the beach (40°36′22″ N latitude, 26°21′28″ longitude E; Fig. 1B) below coquina beds with *Ostrea* and interbedded with *Cardium*-bearing sands of Zanclean Age (Çağatay et al., 1998, 2006). This section probably corresponds to the upper third of the Erikli section of Sakınç et al. (1999) and Sakınç and Yaltırak (2005) that the authors refer to the Alçıtepe Formation. The studied sample of the blue clays includes *Amaurolithus delicatus*, *Braarudosphaera bigelowii*, *Calcidiscus leptoporus*, *Ceratolithus acutus*, *Coccolithus pelagicus*, *Florisphaera profunda*, *Thoracosphaera* sp., *Reticulofenestra pseudoumbilicus*, *Sphenolithus abies* and *Triquetrorhabdulus rugosus*. Reworked specimens are rare. According to the co-occurrence of *C. acutus* and *T. rugosus*, this moderately preserved nannoflora also belongs to the beginning of the nannofossil Subzone NN12b covering an interval from the topmost of the Messinian (after the MSC) up to the early Zanclean (Fig. 3).

3.1.2. Dardanelles Strait

At Burhanlı (40°18′17″ N latitude, 26°33′08″ E longitude; Fig. 1C), six samples from the variegated clays alternating with sands of the Kirazlı Formation provided a moderately preserved nannoflora along 10 m with a continuous record of *Reticulofenestra pseudoumbilicus*, *R. rotaria* and *Triquetrorhabdulus rugosus* (Fig. 5). *Nicklithus amplificus* was recorded in the two uppermost samples. Reworkings from Cretaceous, Eocene, Oligocene and Miocene have been observed. Such an assemblage is considered to represent the upper part of the nannofossil Subzone NN11b and the lowermost part of the nannofossil Subzone NN11c (Fig. 5), i.e. latest Tortonian to early Messinian in age (Fig. 3).

Northward Eceabat (40°11′30″ latitude N, 26°21′18″ E longitude; Fig. 1C), four samples have been studied from the whitish clayey base (20 m thick) belonging to the Kirazlı Formation, and one sample (10 m higher) from a clayey intercalation within calcareous tabular deposits of the Alçıtepe Formation (Sakınç et al., 1999). All of them display a nannoflora characterized by a poor to moderate preservation and few reworked specimens. It includes *Amaurolithus primus*, *Reticulofenestra pseudoumbilicus*, *R. rotaria* (samples 1, 2, 4, 5), *Nicklithus amplificus* (samples 1 and 3) and *Triquetrorhabdulus rugosus* (Fig. 6). Such an

assemblage belongs to the NN11c nannofossil Subzone (Fig. 6), early Messinian in age (Fig. 3).

In the nearby Poyraztepe hill (40°12′27.6″ N latitude, 26°21′59.9″ E longitude; Fig. 1B), the upper part of the section belonging to the Alçıtepe Formation and with a stratigraphic position higher than the top of the Eceabat section, provided a nannoflora from its uppermost clayey intercalations (two samples) just underlying the topmost limestone. These samples contain, among an important amount of reworked specimens from Eocene to Lower Miocene, *Triquetrorhabdulus rugosus* and *Reticulofenestra pseudoumbilicus*, without any specimen of *Reticulofenestra rotaria* or *Nicklithus amplificus* (Fig. 7). Taking into account their stratigraphic position (see above) and the absence of the latter species, we consider that these samples belong to the NN11d Subzone (Fig. 7), i.e. the late Messinian, and more precisely to the first step of the MSC with respect to the importance of reworking (Fig. 3).

Near Kilitbahir, two sections were investigated: the one on the seashore (40°10′08.8″ E longitude, 26°22′16″ N latitude) belongs to the Kirazlı Fm. and that along a path above the castle (40°08′35″ E longitude, 26°22′10″ N latitude) to the Alçıtepe Fm. (Sakınç et al., 1999; Sakınç and Yaltırak, 2005) (Fig. 1C) where we took one sample. The coastal locality is made of 1.50 m of blue clays rich in mollusc shells where three samples were taken overlain by about 20 m of sands including, 4 m over their base, a blue clayey bed (1 m thick) which provided one sample. The three lowermost samples contain *Triquetrorhabdulus rugosus* and *Reticulofenestra pseudoumbilicus* (Fig. 8); additionally, huge Eocene to Lower Miocene reworked nannofossils are present. The sample 4 (from the intercalated clays of the Kilitbahir seashore section) contains, besides the above-mentioned taxa, *Ceratolithus acutus*; a similar nannofloral assemblage with *C. acutus* and *T. rugosus* was identified in the sample Kilitbahir castle (Fig. 8). The two samples yielding *C. acutus* are characterized by a weak reworking. They belong to Subzone NN12b (Fig. 8), i.e. the extreme end of Messinian to earliest Zanclean (Fig. 3). The three coastal samples belong to Subzone NN12a, i.e. to the latest Messinian (Fig. 3). As it has been demonstrated that the Mediterranean reflooding anticipated the base of the Zanclean Stage (Popescu et al., 2007, 2009) as defined by its GSSP (Global Stratotype and Point Section: Van Couvering et al., 2000) and in the absence of any unconformity between samples of Subzones NN12b and NN12a, we consider that all these samples immediately postdate the MSC (Fig. 3).

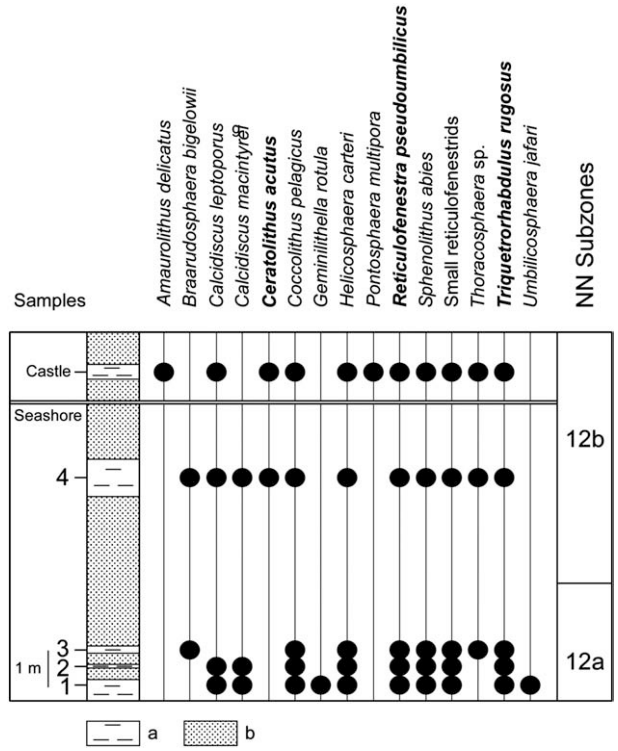

Fig. 8. Distribution and biostratigraphy of the calcareous nannofloras from the Kilitbahir seashore and castle localities. Nannoplankton biostratigraphic markers are in bold characters. a, Clay; b, Sand.

At the beach of Seddülbahir, there are two distinct sections both referring to the Alçıtepe Fm. (Sakınç and Yaltırak, 2005), of which the second section constitutes the reference exposure: (1) to the East (40°02′30″ N latitude, 26°11′12.1″ E longitude; Fig. 1C), a thin section

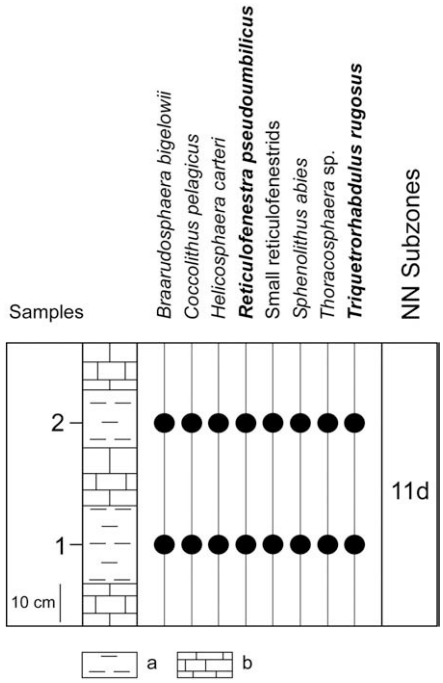

Fig. 7. Distribution and biostratigraphy of the calcareous nannofloras from the Poyraztepe locality. Nannoplankton biostratigraphic markers are in bold characters. a, Clay; b, Limestone.

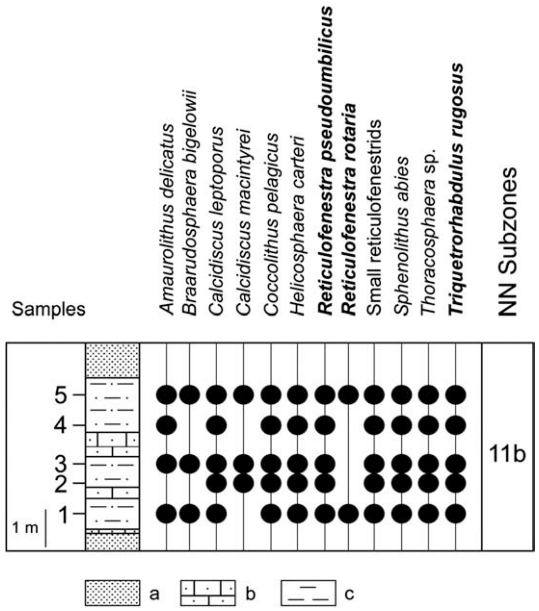

Fig. 9. Nannoflora of the East Seddülbahir locality with indication of nannoplankton subzone. Nannoplankton biostratigraphic markers are in bold characters. a, Sand; b, Sandstone; c, Clay.

(5 m thick) mostly made of sands, clays and marls, yielded within five samples nannofloral assemblages with *Triquetrorhandulus rugosus*, *Reticulofenestra pseudoumbilicus* and *R. rotaria* (Fig. 9), that we refer to the Subzone NN11b (Fig. 9), i.e. latest Tortonian–earliest Messinian in age; notably, *Nicklithus amplificus* does not occur (Fig. 3); (2) to the West (40°02′38″ N latitude, 26°10′55″ E longitude; Fig. 1C), the second section, made of thick clays (about 30 m) rich in mollusc shells, provided nannofloras containing as significant biostratigraphical taxa *Triquetrorhabdulus rugosus* and *Reticulofenestra pseudoumbilicus* and, additionally, *Ceratolithus acutus* in the topmost 11 m (samples 8–12; Fig. 10). Reworking is weak. As there is no unconformity within the West Seddülbahir section, we may suppose that the nannofloral assemblages evidence a continuous passing from Subzone NN12a to NN12b (Fig. 10), i.e. from the latest Messinian (after the peak of the MSC, as at the Kilitbahir seashore section) to the earliest Zanclean (Fig. 3). However, the West Seddülbahir section is obviously discordant over the East Seddülbahir one.

The Intepe section (40°1′27″ N latitude, 26°20′33″ E longitude; Fig. 1C) (Gillet et al., 1978; Sakınç and Yaltırak, 2005) is about 77 m thick, of which we studied the 36 m thick central part (Fig. 11A, C). The studied section is made up of sands, clays, calcareous sandstones and thin limestones. It is topped by yellow sands and pebbly sandstones and a thick calcareous flagstone which constitutes a local reference surface.

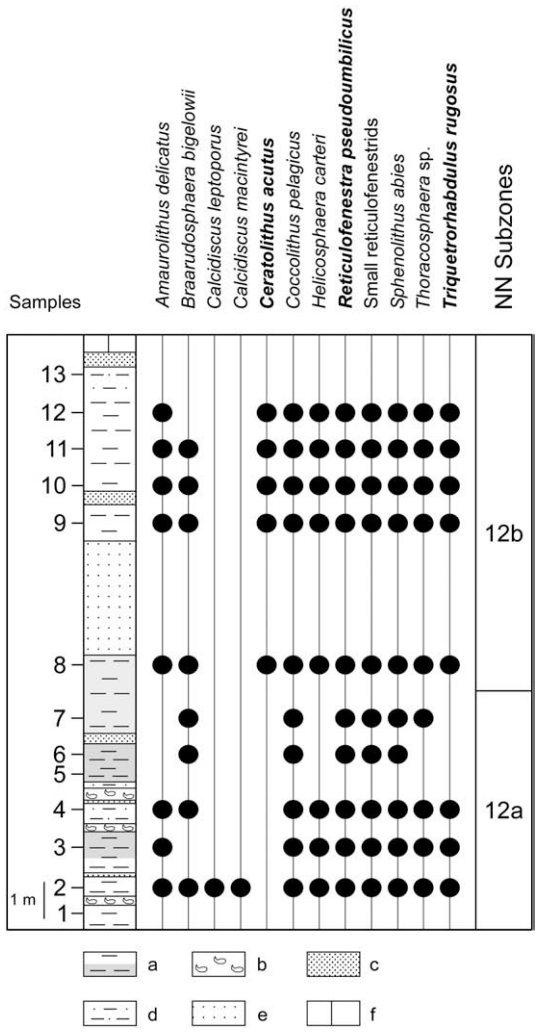

Fig. 10. Distribution and biostratigraphy of the calcareous nannofloras from the West Seddülbahir locality. Nannoplankton biostratigraphic markers are in bold characters. a, Dark-light clay; b, Coquina; c, Sand; d, Silt; e, Sandstone; f, Limestone.

The section is rich in *Mactra* shells and displays also gastropod shells such as *Melanopsis*. In its middle part, the section displays a thin lignite (5 cm thick) (Gillet et al., 1978) overlain by a sand (2 cm thick) and a *Mactra* coquina (17 cm thick) (Fig. 11B–E). Thirty five samples were studied: all of them provided a relatively well-preserved nannoflora (Fig. 12). From the biostratigraphic point of view, *Amaurolithus primus* was discontinuously present all along the section, *Reticulofenestra rotaria* was found in samples 14–18, *Nicklithus amplificus* in samples 1 and 7, *Triquetrorhabulus rugosus* almost continuously recorded from sample 1 to sample 31, *Ceratolithus acutus* regularly from sample 24 to sample 35 (Fig. 12). Hence, the lower part of the studied section (samples 1–18) belongs to the NN11c calcareous nannofossil Subzone according to the joint occurrence of *R. rotaria* and *T. rugosus* and the occasional presence of *N. amplificus*, while its upper part (i.e. from sample 24 where *C. acutus* appears) represents a large part of Subzone NN12b including the disappearance level of *T. rugosus* (Fig. 12). As a consequence, the interval between samples 18 and 24 belongs to the NN11c Subzone and maybe to NN12a Subzone for the uppermost layers just preceding sample 24 (Fig. 12). Distinction between Messinian and Zanclean can be placed around samples 23–24 according to the first appearance level of *Ceratolithus acutus*. If some changes in sea-level have been recorded in the section with respect to an impact of the MSC, they concern the layers immediately underlying the appearance of *C. acutus* (Fig. 12). Our research focussed on the lignite corresponding to our sample 21 (Fig. 11C–D) as a first candidate because of its deposition under few centimetres of water. The lignite has an erosional contact with the overlying fine sand (Fig. 11E). But the expected gap in sedimentation is obvious in a lateral outcrop where the lignite is directly overlain on a long distance by reddish clays indicative of an emersion phase (Fig. 11F), because in present-day lignite quarries, lignites catch fire readily upon exposure, firing the overlying clays, thus producing 'porcellanite' (Fig. 11G). This is the obvious signature of an emersion event that occurred just below the appearance of *C. acutus*. Accordingly, we may consider that (1) the lignite corresponds to the first step of the MSC (5.960–5.760 Ma; Fig. 3) characterized by a weak fall in sea-level (ca. 150 m), (2) the immediately overlying clays correlate with the sea-level rise separating the two steps of the MSC (5.76–5.60 Ma; Fig. 3), (3) the erosion of these clays or their firing (when being partly preserved during the duration of exposure) signs the huge drop in sea-level (ca. 1500 m) of the peak of the MSC (5.60–5.46 Ma; Fig. 3) (Clauzon et al., 1996).

About 34 m thick, the Yenimahalle section (39°57′51″ N latitude, 26°17′46″ E longitude; Fig. 1C), is mostly composed of sands, sandstones and limestones including some clayey intercalations. It was described by Çağatay et al. (2006) who included it into the Alçıtepe and Truva formations. Palaeomagnetic measurements performed here by W. Krijgsman (Çağatay et al., 2006) revealed a continuous reverse signal and the section was assigned to Chron C3r, and more precisely to its Messinian part. However, the Yenimahalle section should be relatively younger than the Intepe section because it overlies an obvious morphological surface atop the Intepe section, an assumption also supported by the absence of any calcareous coccolith at Yenimahalle. *Ceratolithus acutus* is recorded without *Triquetrorhabdulus rugosus* in the upper part of the Intepe section (Fig. 12) which could belong to the uppermost part of Chron C3r, and possibly Chron C3n.4n (see Fig. 3). As a consequence, the Yenimahalle section should be assigned at least to the next reverse chron, i.e. Chron C3n.3r (Fig. 3).

The Truva section (39°57′30″ N latitude, 26°14′47″ E longitude; Fig. 1C), with a thickness of only 5 m, and composed of limestones and intercalated clays, overlies the Yenimahalle section (Fig. 3) and tops the Truva Fm. No calcareous nannoplankton was found in the two studied samples.

The above-presented results, based on calcareous nannoplankton investigations, allow us to date in detail several Upper Miocene–Lower Pliocene reference sections from NW Turkey, and also to identify in detail a succession of nannofloral events the time-interval encompassing the MSC (Fig. 3). Particularly, the first record of *Ceratolithus acutus* in

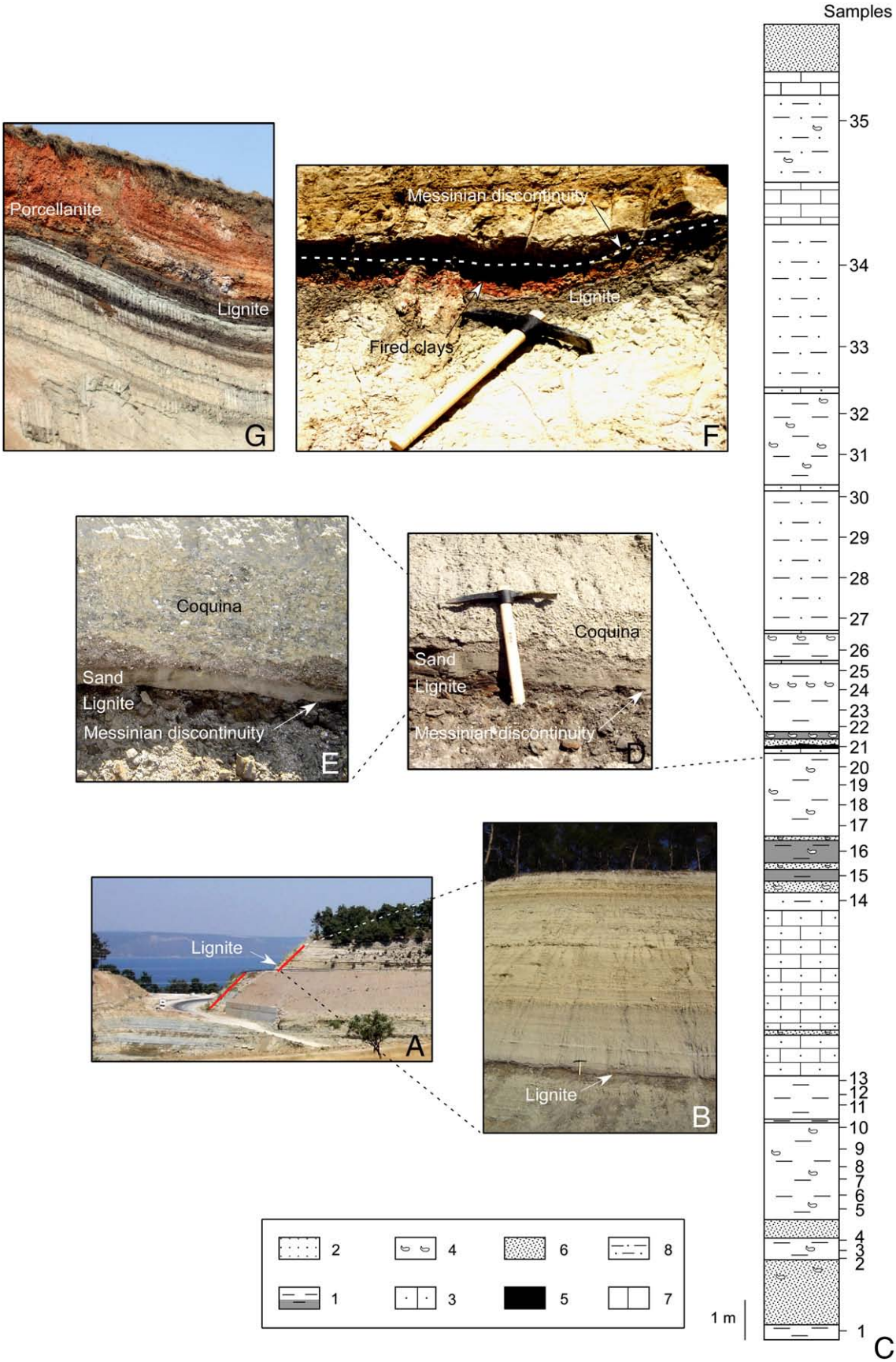

Fig. 11. Lithostratigraphy of the central part of the Intepe section. A, General view of the Intepe section where red lines indicate the studied (i.e. central) part of the section; B, Upper part of the studied section; C, Lithological log of the studied section, location of samples; 1, Dark-light clay; 2, Sand; 3, Calcareous sandstone; 4, Mollusc shells; 5, Lignite; 6, Sandstone; 7, Limestone; 8, Silt. D, Lignite-coquina interval including the discontinuity caused by the peak of the MSC; E, Detail of Fig. 4D; F, Fired clays (porcellanite) overlying the lignite and marking the discontinuity caused by the peak of the MSC; G, Present-day analogue from the S Romania lignite Lupoaia quarry showing clays transformed into porcellanite after being naturally fired by the underlying lignite. (For interpretation of the references to colour in this figure legend, the reader is referred to the web version of this article.)

the Kilitbahir, West Seddülbahir and Intepe sections may reliably be considered as corresponding practically to its first appearance datum. This event is well-calibrated in the global ocean at 5.345 Ma (Raffi et al., 2006), i.e. slightly after the end of the peak of the MSC, estimated at 5.46 Ma by Clauzon et al. (2008). At Kilitbahir and West Seddülbahir, *C. acutus* was recorded for the first time few metres above the Messinian Erosional Surface (Figs. 8 and 10), i.e. in a consistent chronostratigraphic position with its global first appearance datum. The same situation concerns the Intepe section, where the first occurrence of *C. acutus* has been found slightly above the Messinian discontinuity which corresponds to the Messinian Erosional Surface in an embayment context (Fig. 12). The nannofloral scarcity of some layers (i.e., samples 24 and 25; Fig. 12) does not constitute an impediment for biostratigraphical interpretations; probably these layers correspond to a restrictive environment, such as a lagoonar one, as it is suggested in the next section of "Palaeoenvironment reconstructions".

3.2. Palaeoenvironmental reconstructions

We particularly considered palynomorphs, mainly those from the Intepe section where we focussed on the interval encompassing the MSC: (1) the dinoflagellate cysts for the coastal marine environment reconstruction, and (2) the pollen grains for the vegetation, climate and palaeoaltitude reconstruction. We also took into account the calcareous nannoplankton, a group of marine algae which live in marine surface waters (0–200 m), being therefore affected by changes in the surface water environment, particularly salinity, temperature and nutrient availability.

3.2.1. Coastal marine palaeoenvironments

The dinoflagellate cyst flora from the Intepe section comprises only 12 taxa, to which can be added freshwater algae *Pediastrum* and *Botryoccocus* colonies that are interpreted as markers of freshwater input (Fig. 13). Preservation of dinoflagellate cysts is poor to moderate. The dinoflagellate cyst assemblage is constituted by: (1) oceanic species and other neritic species as *Spiniferites mirabilis* and *S. membranaceus*, (2) marine autotrophic cosmopolitan species such as *Lingulodinium machaerophorum*, *Operculodinium centrocarpum* sensu Wall and Dale, *Spiniferites bentorii*, *S. bentorii* subsp. *truncates*, *S. hyperacanthus*, *S. ramosus*, *S. bulloideus*, *Spiniferites* spp., and (3) Paratethyan brackish species as *Galeacysta etrusca* and *Impagidinium globosum*. Despite dinoflagellate cyst scarcity, their assemblage distribution, completed by the relative frequency of freshwater algae documents palaeoenvironmental changes.

During the time-interval covered by the samples 15–19, the dinoflagellate cyst flora was dominated by marine euryhaline species as *O. centrocarpum*, *L. machaerophorum*, *Spiniferites bulloideus*, *S. ramosus*, *S. bentorii*, *S. bentorii* subsp. *truncates* and *S. hyperacanthus*. The high relative abundance of *Spiniferites* spp. (more than 50%), characterized by short processes, denotes the deterioration of marine conditions, in relation with a drop in salinity (Kokinos and Anderson, 1995; Hallett, 1999; Ellegaard, 2000; Sorrel et al., 2006; Popescu et al., 2009). Notably is the presence of *S. mirabilis* within sample 15 (one specimen), and that the presence of the Paratethyan brackish dinoflagellate cysts *Galeacysta etrusca* in sample 17 (one specimen) and *Impagidinium globosum* in samples17 and 19 (one specimen per sample). Morphology of *G. etrusca* denotes that this specimen belongs to the morphological group "C" (small endocyst/exocyst ratio) of Popescu et al. (2009).

Samples 20 to 23 are characterized by the absence of dinoflagellate cysts and a huge increase (acme) of *Pediastrum* that indicates a new change in the local environments marked now by fresh- to brackish-water conditions. Salinity at that time is probably less than 4.6 pps, according to minimum of salinity tolerance of *S. ramosus* (Marret and Zonneveld, 2003), identified as the most tolerant marine eurihaline species within the Intepe assemblage. This interpretation is consistent with the absence of calcareous nannoplankton and deposition of a lignite layer (sample 21) when shallow water and freshwater conditions prevailed. *Pediastrum* was also found in sample 24, with a high relative abundance indicating continuous fresh- to brackish-water conditions, sometimes interrupted by incursions of marine waters. Sample 25 is characterized by the increase in diversity of marine dinoflagellate cysts and their relative abundance in opposition to a decrease of *Pediastrum*, that indicates increased salinity. Sample 26 is characterized by the absence of marine dinoflagellate cysts and increase of freshwater algae, which marked the return of prevalent freshwater input.

According to the dinoflagellate cyst record, we may propose a relatively detailed evolution of the environmental conditions during the time-interval corresponding to samples 15–26, as summarized:

- from samples 15 to 19, the local environment was characterized by low saline conditions that evolved progressively to brackish ones at the top of the interval; this decrease in salinity of surface waters caused unfavourable conditions for marine plankton;
- samples 20 to 23 indicate an huge input of freshwater resulting in brackish to freshwater conditions in the local environment, sometimes interrupted by some marine incursion revealed by the calcareous nannoplankton;
- samples 24 and 26 display the progressive increase in salinity in relation with the reflooding by marine waters and some freshwater inputs.

The nannoflora is on the whole consistent with the information from the dinoflagellate cyst assemblages. It is to be noticed that the nannoplankton diversity is drastically altered in samples 21–23, while it was high in the lower part of the studied section (especially in the interval covered by the samples 5–13), being again considerably reduced in its upper part (samples 31–35) (Fig. 12). Notably, the nannofossil *Braarudosphaera bigelowii* and the calcareous dinoflagellate *Thoracosphaera* have a more consistent frequency within samples 8–13 than in lower levels, indicating stressfully conditions in relation probably with the drop in salinity. At the beginning of the interval covered by the samples 14–21, a significant increase of the calcareous dinoflagellate *Thoracosphaera* was observed. *Thoracosphaera* decreases at the top of the above-mentioned interval; its lowermost abundance corresponds to the highest frequency of *B. bigelowii*. The significant decrease of *Thoracosphaera*, coincident with the *B. bigelowii* bloom, is probably indicative of an important decrease in salinity. The collapse of the calcareous nannofossil assemblage and the progressive decrease in salinity possibly mirrored the transition from a hyposaline (even brackish) environment to a continental one, marked by the deposition of the lignite layer. Between samples 22 and 26, *B. bigelowii* represents a minor component of the nannoflora. *Thoracosphaera*, after a peak recorded at the base of this interval, drops significantly. In the uppermost part of the section (samples 27–35), *B. bigelowii* and *Thoracosphaera* represent minor component of the assemblages.

Finally, considering both the dinoflagellate cysts from samples 15–26 and the nannoplankton all along the section, three main ecostratigraphic intervals have been identified within the studied part of the Intepe section (earlier first):

- (1) samples 1–13, denoting almost normal marine conditions;
- (2) samples 14–21, illustrative of a sea-level fall associated with a decrease in salinity (probably brackish conditions), and some emersion at the top;
- (3) samples 22–35, indicating a return to almost normal marine conditions in spite of some deterioration in the uppermost layers.

3.2.2. Continental palaeoenvironments

Fourteen samples from the Dardanelles Strait area provided pollen grains in sufficient quantity. They inform on the vegetation and climate of the region just before and after the MSC. Herbs (Asteraceae, Poaceae, Amaranthaceae–Chenopodiaceae, Caryophyllaceae, *Artemisia*, etc.)

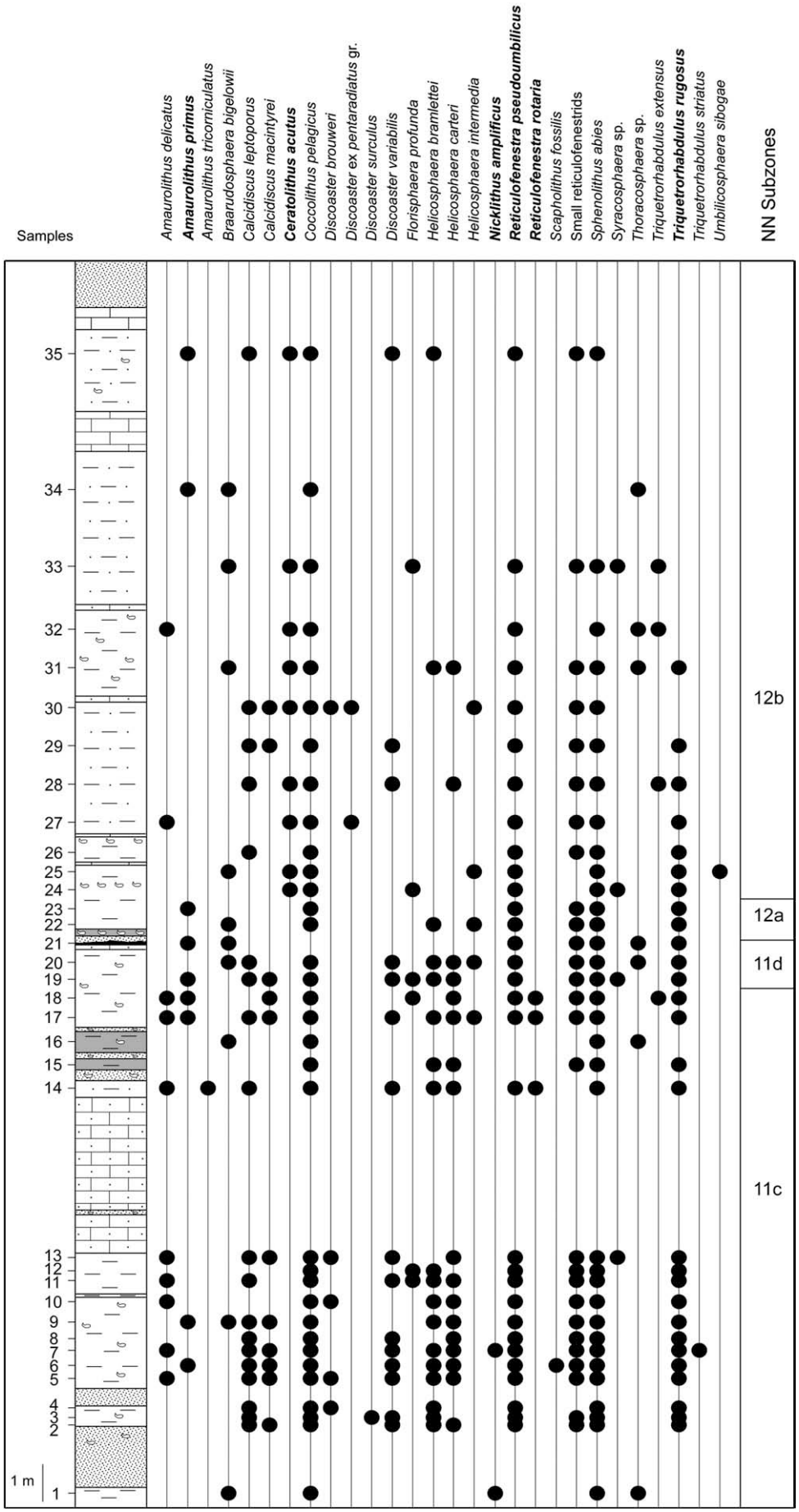

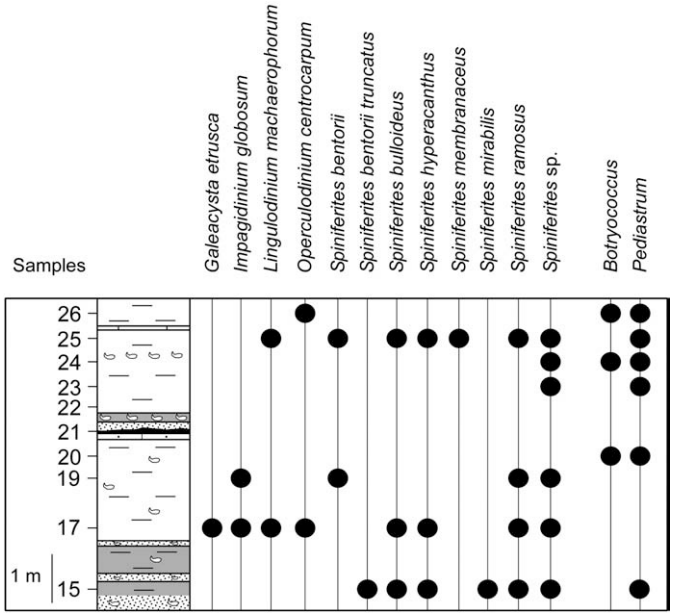

Fig. 13. Dinoflagellate cyst flora from eight samples of the central part of the Intepe section. Lithological legend, see Fig. 11.

predominated before the MSC (in the sections Burhanlı, Eceabat, Intepe *p.p.*), while trees were mostly composed of warm-temperate elements (*Quercus*, *Carya*, *Zelkova*, etc.) with few subtropical elements (Taxodiaceae, *Engelhardia*) (Fig. 14). Sample 21 shows important halophytes plus an over-representation of aquatic plants (*Potamogeton*, *Typha*, *Myriophyllum* and *Sparganium*), the reason for which it was not draft on Fig. 14. It denotes a coastal freshwater marsh. After the MSC (Intepe *p.p.*, Seddülbahir), subtropical trees (with *Cathaya*) show larger percentages as *Pinus* and altitudinal trees (*Cedrus*, *Abies* and *Picea*) do (Fig. 14). Increase in disaccate pollen grains (*Pinus*, *Cedrus*, *Abies* and *Picea*) could indicate a more distal location of the upper part of the Intepe section with respect to the palaeoshoreline, i.e. in relation with marine water invasion after the MSC. However, the larger representation of halophytes (Amaranthaceae–Chenopodiaceae) and freshwater plants (*Sparganium*, Alismataceae, *Potamogeton*) after the MSC points out nearby coastal environments.

As a consequence, we suggest that the increase in conifer pollen grains (*Cedrus* mainly, with *Abies* and *Picea*) could be significative of some relief uplift resulting in a larger representation of altitudinal conifers in coastal pollen records. Southward Intepe, the Kayacı Mount which is made of Eocene–Oligocene volcanic rocks does not bear evidence for uplift during the latest Miocene. *Cedrus* does not like silice-rich soils but prefers limestones, dolomites and flysch (Quézel, 1998; Quézel and Médail, 2003). Hence, the Kayacı relief, whatever its elevation, is not a likely source of *Cedrus* pollen grains. Armijo et al. (1999) suggested that the Ganos–Gelibolu Mountain, situated to the North of the Dardanelles and mostly constituted by Eocene–Oligocene flysch and volcanics, has been uplifted during the Messinian as a response to the propagation of the North Anatolian Fault (Fig. 1B). This relief appears to be a good candidate for the habitat of *Cedrus* forests as they exist today in southern Turkey (Quézel, 1998; Quézel and Médail, 2003). Uplift occurred during the late Messinian, fact also suggested by the significant percentages in *Cedrus* plus *Abies* and *Picea* recorded at Intepe section after the MSC (samples 22–26) unlike for the older deposits (in the sections Burhanlı, Eceabat and in the section Intepe in samples 15–20) (Fig. 14). Reconstruction of the mean annual temperature by palaeoclimatic transfer function (Fauquette et al., 1998) in the coastal area using a selection of the pollen assemblage (altitudinal trees are not employed for this calculation) offers a possibility to estimate minimum palaeoaltitude of the nearby massif (Fauquette et al., 1999) as altitudinal elevation of conifer belts is narrowly linked to temperature and, as a consequence, to latitude of the massif (Ozenda, 1989). This estimate was done using the pollen record of Intepe after the MSC. The most probable mean annual temperature calculated for the Intepe samples 22–26 is 16.5 °C (range: 15–18.5 °C). This temperature is recorded today, in Turkey at low altitude, at around 38.5° of North latitude. We applied the method described by Fauquette et al. (1999) where the estimated palaeotemperatures are shifted into present-day latitudes. The obtained latitudes are projected onto the altitudinal elevation gradient of the *Abies–Picea* belt with respect to decreasing latitude (100 m in altitude per degree in latitude; Ozenda, 1989) and provide a range from 1800 to 2400 m for the minimum altitude of the Ganos Mountain with a most probable value at 2000 m.

4. Discussion

The new bio- and ecostratigraphic data provide consistent information on the impact of the MSC in the Dardanelles which must be discussed in terms of palaeogeographic inferences and palaeoenvironments.

4.1. Palaeogeographic inferences

This study allows to date precisely some key-sections defining the regional stratigraphic framework, which was previously established by rather loose correlations of lithological units, using mollusc macrofossils which may have a large range of salinity tolerance and duration (Sakınç et al., 1999).

The most important outcome concerns the Alçıtepe Fm. which is younger than the Messinian Salinity Crisis according to its two reference sections:

- at Seddülbahir, the Alçıtepe Fm. deposits (i.e. the West Seddülbahir section) are separated from the Kirazlı Fm. deposits (i.e. the East Seddülbahir section) by an angular unconformity which hence corresponds to the Messinian Erosional Surface (Fig. 15B, C);
- at Intepe, the Alçıtepe Fm. deposits conformably overlie those of the Kirazlı Fm., but we infer an unconformity between the two formations, resulting from emersion and probably some erosion in relation with the peak of the MSC, this is what we called the Messinian discontinuity (Figs. 11 and 15B).

In addition, the Eceabat section plus its uppermost part at Poyraztepe hill, which were conventionally attributed to the Alçıtepe Fm. on the basis of lithological similarities, have a late Messinian Age and must belong to the Kirazlı Fm. (Figs. 3 and 15B, D). Beds of the Eceabat and Poyraztepe sections dip 10–15° NW and culminate at altitude 143 m (Fig. 15D). Southward, between Eceabat and Kilitbahir (Fig. 15D), sediments younger than the MSC start from the seashore and relate to the early Zanclean up to the altitude 125 m where calcareous nannoplankton (*Triquetrorhabdulus rugosus* and *Ceratolithus acutus*) was recorded above the Kilitbahir castle (Figs. 3 and 15B, D, G). As they are covered by the Alçıtepe calcareous flagstone, they are obviously nested within the Messinian succession of Eceabat–Poyraztepe from which they are necessarily separated by the Messinian Erosional Surface (Fig. 15B, D) that can be observed along the road southward Eceabat. The extremity of the Gelibolu Peninsula obviously corresponds to the sedimentary filling of a fluvial valley incised during the peak of the MSC (Fig. 15A), as suggested by Armijo et al. (1999). Many places in this area, such as at Nuriyamut (Fig. 15A,

Fig. 12. Distribution and biostratigraphy of the calcareous nannofloras from the Intepe section. Nannoplankton biostratigraphic markers are in bold characters. Lithological legend, see Fig. 11.

B), show thick early Zanclean sands with gravels with an organization in foreset beds dipping (25–30° at Nuriyamut) in the direction of the axis of the Messinian valley (Fig. 15F). Such a sedimentary organization is typical of a Gilbert-type fan delta which is the widespread feature of sediments within the Messinian canyons after the Mediterranean reflooding (Clauzon, 1990; Clauzon et al., 1990). Clayey deposits at West Seddülbahir and Kilitbahir seashore constitute the bottomset beds of the Dardanelles Gilbert-type fan delta more or less imbricated with coarser foreset beds (Fig. 15B). The calcareous topmost plateau of Alçıtepe constitutes the abandonment surface of the Gilbert-type fan delta.

On the southern coastline of the Dardanelles Strait, the horizontal sediments observed in the Intepe section are suddenly (300 m northward the section) replaced by sands and gravels organized in foreset beds dipping (25°) in direction of the Dardanelles Gilbert-type fan delta (Fig. 15E). The contact is obviously erosional as it has been precisely followed on land back to the Güzelyalı village (Fig. 15A). This Gilbert-type fan delta construction fills a canyon cut by a tributary of the main Dardanelles fluvial drain during the peak of the MSC (Fig. 15A, B). Here, the Messinian Erosional Surface incises deposits of the Kirazlı Formation and laterally evolves into a discontinuity in an interfluve context (Intepe section) as drawn on Fig. 15B.

Accordingly, the impact of the MSC is obvious in the region and must henceforth be considered in the stratigraphic setting and palaeogeographic reconstructions. The gap in sedimentation because of erosion (Dardanelles and tributary Messinian canyons) or non-deposition (Intepe) is chronostratigraphically located in the extremely latest Messinian, i.e. during the peak of the MSC, and not in the Zanclean as repeatedly assumed as by Sakınç et al. (1999) and Sakınç and Yaltırak (2005). Nesting of post-MSC deposits within the pre-MSC ones must allow distinguishing the Alçıtepe Formation from the Kirazlı Formation without using the often misleading facies characteristics.

In the Gulf of Saros, nesting of the post-MSC sediments within the older ones is not very pronounced, probably because of a relatively weak fluvial activity. The most intense fluvial activity during the MSC was located in the Dardanelles Strait area; it rapidly diminished when passing to an interfluve context, as supported by the palaeoenvironmental data.

In spite of its reverse palaeomagnetic signal and the record of Paratethyan organisms, the Yenimahalle section cannot be considered as representative of the MSC in the region. Clearly overlying the topmost flagstone of Intepe, which has a similar significance as the abandonment surface of the Dardanelles Gilbert-type fan delta, the Yenimahalle section has a younger Zanclean Age and represents the end of the Pliocene sedimentation in the region (Fig. 15B).

4.2. Palaeoenvironments

The present-day southern shoreline of the Dardanelles Strait is a key-area because of the proximity of distinct environments during the peak of the MSC (a fluvial canyon and an interfluve domain) and after it (a subaquatic delta system and a coastal domain). Such an environmental coexistence is somewhat normal but the accuracy of its record over a short distance is infrequent. At Intepe, the local environment fluctuated between marine and almost freshwater conditions in relation with moderate to intense fluvial freshwater inputs. The blooms of the calcareous dinoflagellate *Thoracosphaera* are situated at the base and towards the top of the interval, and may be associated with the calcareous nannoplankton collapse (Fig. 12). Such blooms may reflect unstable marine conditions, associated with an important nutrient record (possibly linked to a high terrigenous input) and the lack of other marine planktonic competitors. The bloom of the calcareous nannoplankton species *Braarudosphaera bigelowii* at the top of the Messinian layers at Intepe is probably related to the salinity fluctuations. As they are highly sensitive to environmental changes, dinoflagellate cysts require that the Intepe locality was very close to the paleoshoreline. A bay head (Fig. 15A) seems to be the probable palaeogeography before and after the MSC while the varying freshwater inputs depended from the nearby river. Such a relatively isolated context was significantly impacted by the successive fluctuations in Mediterranean sea-level and the resulting steps of the MSC (Clauzon et al., 1996). The moderate sea-level fall of the first step of the MSC is marked by the lignite and development of marsh conditions (5.96–5.76 Ma: Fig. 3). The following sea-level rise is indicated by the overlying clays (5.76–5.60 Ma: Fig. 3), mostly eroded or fired during the episode of emersion corresponding to the huge sea-level drop of the peak of the MSC during which the nearby fluvial canyon was cut (5.60–5.46 Ma). Climatic conditions are warm and relatively dry out of the riverbanks, as it is indicated by the large percentages of herb pollen grains. Some relief uplifted during the MSC, event probably connected to the establishment of an important relief in the Ganos–Gelibolu Massif.

According to these results, we may address questions about the gateway between the Black Sea (i.e. the Eastern Paratethys domain) and Aegean Sea (the Eastern Mediterranean domain) through the

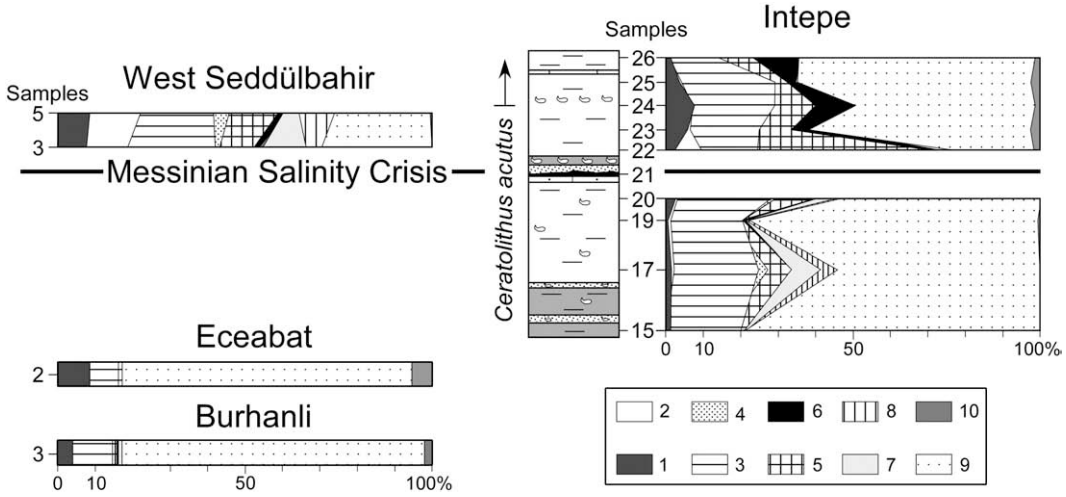

Fig. 14. Synthetic pollen diagram from some localities before and after the peak of the MSC. 1, Subtropical trees; 2, *Cathaya*; 3, Warm-temperate trees; 4, Cupressaceae; 5, Cool-temperate trees (*Cedrus* mainly); 6, Boreal trees (*Abies* and *Picea*); 7, Elements without signification; 8, Mediterranean xerophytes; 9, Herbs; 10, Steppe elements (*Artemisia* mainly).

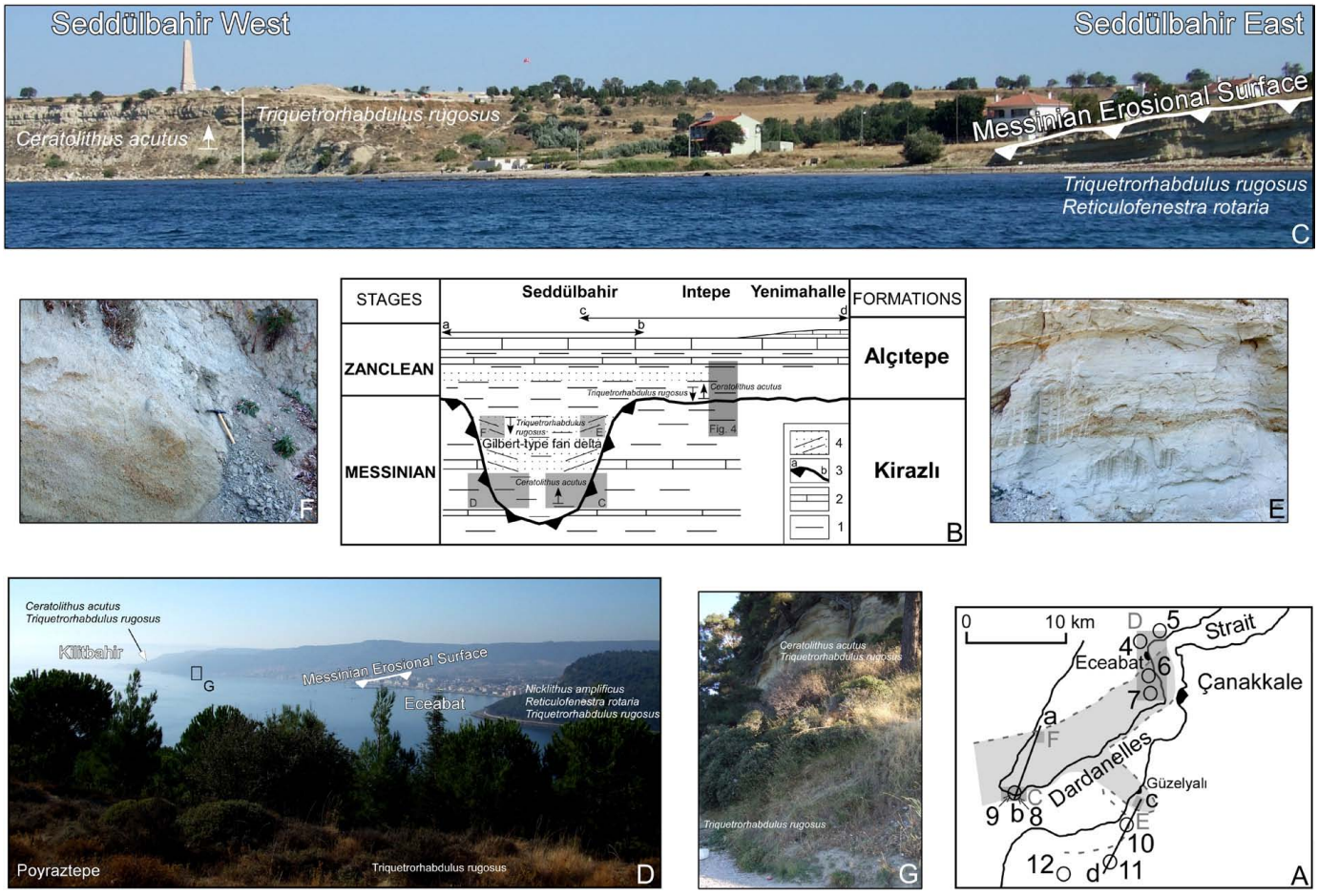

Fig. 15. The Messinian fluvial canyon in the western part of the Dardanelles Strait. A, Map showing the main Messinian fluvial canyon and a tributary (grey surface), the Early Zanclean coastline (dotted grey line), and location of photographs C–F. Sections: 4, Eceabat; 5, Poyraztepe; 6, Kilitbahir (seashore); 7, Kilitbahir (castle); 8, East Seddülbahir; 9, West Seddülbahir; 10, Intepe; 11, Yenimahalle; 12, Truva. B, Reconstructed composite cross-section (a–b, c–d) in the Dardanelles Strait and the extremity of the Gelibolu Peninsula through the Zanclean Gilbert-type fan delta with calcareous nannoplankton events and location of photographs C–F and Fig. 4. 1, Clay; 2, Limestone; 3a, Messinian Erosional Surface; 3b, Messinian discontinuity; 4, Sandy and gravelly foreset beds. C, Photograph of the beach of Seddülbahir showing the Messinian Erosional Surface cutting the clays and sands of the East Seddülbahir section and overlain by the clayey bottomset beds of the West Seddülbahir section. Nannoplankton markers are indicated. D, View of the surroundings of Eceabat showing the Alçıtepe Formation deposits nested within the Eceabat–Poyraztepe sections now reported to the Kirazlı Formation. Nannoplankton markers and the Messinian Erosional Surface are indicated. E, Sandy and gravelly foreset beds near the Intepe section. F, Sandy and gravelly foreset beds at Nuriyamut. G, Kilitbahir (seashore) section with calcareous nannoplankton markers.

Marmara realm during the MSC (Görür et al., 1997; Çağatay et al., 2006) cannot be perpetuated. Indeed, a connection between these domains is incompatible with coeval subaerial erosion both on the Black Sea side (Gillet et al., 2007) and the Dardanelles area (this work) during the peak of the MSC. Connection would have been only possible during times of high sea-level, i.e. before and after the peak of the MSC (Clauzon et al., 2005) or before its first step. However, the extreme scarcity of Paratethyan dinoflagellate cysts in the Intepe sediments does not support such a connection; as these organisms live on the surface waters, we may suppose that a sea-level high-stand should be expressed in their significant increase. For the same reason, a one-way passage resulting in influx of Paratethyan organisms only into the Mediterranean realm (see discussion in: CIESM, 2008) is also questionable. Still, the almost continuous presence of the Paratethyan bivalves and ostracods before and after the MSC in the region (Çağatay et al., 2006) needs to be explained. It has been suggested that their arrival was caused by an episode of high sea-level just before the peak of the MSC (Clauzon et al., 2005; Popescu et al., 2009) and that their persistence was favoured in some relatively isolated environments (lagoons, bays) at the frontier between marine, brackish and fresh-water conditions (Çağatay et al., 2006). But, as we mentioned above, the Paratethyan dinoflagellate cysts (which should be the earliest immigrants as planktonic organisms) are absent or extremely rare in our samples, and therefore do not support the hypothesis of a connection allowing the penetration of the Paratethyan macrofaunas throughout a Marmara marine corridor, connecting the Black Sea (i.e. the Eastern Paratethys domain) and the Aegean Sea (the Eastern Mediterranean domain) during the MSC.

5. Conclusion

The chronological constraints presented in this work provide a sound background for new prospects on the late Miocene–Pliocene stratigraphy and palaeogeography in the Dardanelles region. Evidence of the strong impact of the MSC in the region, as elsewhere around the Mediterranean, indicates that the Dardanelles Strait was a fluvial collector eroding the older rocks during the peak of the MSC. The systematic use of the calcareous nannoplankton biostratigraphical results in a clarified regional stratigraphy, unbiased by lithological similarities. In this region as everywhere around the Mediterranean, the peak of the MSC and the resulting erosional surface or discontinuity may be regarded as a robust chronological indication. The most important results lie in the fact that the Alçıtepe formation is a Pliocene unit postdating the MSC and that the Kirazlı formation is a Late Miocene unit predating the MSC. The study in progresses aims at reconstructing the Messinian fluvial network in the Marmara region and deciphering the role of the MSC on the North Anatolian Fault propagation across the region. Finally, the Dardanelles–Marmara region is to be discarded as a connection between the Black Sea (i.e., the Eastern Paratethys domain) and Mediterranean Sea, during the Messinian Salinity Crisis.

Acknowledgements

This research started within the frame of the CNRS-INSU ECLIPSE II Programme and was mostly developed thanks to the ANR EGEO Project. One of us (D. Biltekin) was granted by the French Embassy in Turkey for her PhD thesis. This paper is a contribution to the Projects IDEI of the Romanian National Programme of Research, Development and Innovation (Projects No. 144/2007 CNCSIS Code 816 and 364/2007, CNCSIS Code 815 — M.C. Melinte-Dobrinescu). We are indebted to Marie-Pierre Aubry, who reviewed this paper and made valuable suggestions and comments, which significantly increase the chron-ostratigraphic and ecostratigraphic inferences of the manuscript. We also appreciate the improvements suggested by an anonymous referee. The English language was improved by Oliver Bazely. This paper is the ISEM contribution no 2009-029.

References

Agusti, J., Oms, O., Meulenkamp, J.E., 2006. Introduction to the Late Miocene to Early Pliocene environment and climate change in the Mediterranean area. Palaeogeography, Palaeoclimatology, Palaeoecology 238, 1–4.

Armijo, R., Meyer, B., Hubert, A., Barka, A., 1999. Westward propagation of the North Anatolian fault into the northern Aegean: timing and kinematics. Geology 27, 267–270.

Armijo, R., Meyer, B., Hubert, A., Barka, A., 2000. Westward propagation of North Anatolian fault into the northern Aegean: timing and kinematics: reply. Geology 28, 188–189.

Backman, J., Raffi, I., 1997. Calibration of Miocene nannofossil events to orbitally tuned cyclostratigraphies from Ceara Rise. Proceedings of the Ocean Drilling Program, Scientific Results 154, 83–89.

Berggren, W.A., Kent, D.V., Swisher III, C.C., Aubry, M.-P., 1995. A revised Cenozoic geochronology and chronostratigraphy. In: Berggren, W.A., Kent, D.V., Aubry, M.-P., Hardenbol, J. (Eds.), Geochronology, Time Scales and Global Stratigraphic Correlation: A Unified Temporal Framework for an Historical Geology. Special Publication — Society of Economic Paleontologists and Mineralogists, vol. 54, pp. 141–212.

Bukry, D., 1975. Coccolith and silicoflagellate stratigraphy, Northwestern Pacific ocean, Deep Sea Drilling Project Leg 32. Initial Reports of the Deep Sea Drilling Project 32, 677–701.

Çağatay, N.M., Görür, N., Alpar, B., Saatçılar, R., Akkök, R., Sakınç, M., Yüce, H., Yaltırak, C., Kuşcu, I., 1998. Geological evolution of the Gulf of Saros, NE Aegean Sea. Geo Marine Letter 18, 1–9.

Çağatay, N.M., Görür, N., Flecker, R., Sakınç, M., Tünoğlu, C., Ellam, R., Krijgsman, W., Vincent, S., Dikbaş, A., 2006. Paratethyan–Mediterranean connectivity in the Sea of Marmara region (NW Turkey) during the Messinian. Sedimentary Geology 188–189, 171–187.

Castradori, D., 1998. Calcareous nannofossils in the basal Zanclean of the Eastern Mediterranean Sea: remarks on paleoceanography and sapropel formation. Proceedings of the Ocean Drilling Program, Scientific Results 160, 113–123.

Chumakov, I.S., 1973. Geological history of the Mediterranean at the end of the Miocene — the beginning of the Pliocene according to new data. Initial Reports of the Deep Sea Drilling Project 13 (2), 1241–1242.

CIESM, 2008. Executive summary. In: Briand, F. (Ed.), The Messinian Salinity Crisis from mega-deposits to microbiology — A consensus report. CIESM Workshop Monographs, vol. 33, pp. 7–28.

Cita, M.B., Ryan, W.B.F., Kidd, R.B., 1978. Sedimentation rates in Neogene deep sea sediments from the Mediterranean and geodynamic implications of their changes. Initial Reports of the Deep Sea Drilling Project 42A, 991–1002.

Clauzon, G., 1973. The eustatic hypothesis and the pre-Pliocene cutting of the Rhône Valley. Initial Reports of the Deep Sea Drilling Project 13 (2), 1251–1256.

Clauzon, G., 1978. The Messinian Var canyon (Provence, Southern France) — paleogeographic implications. Marine Geology 27, 231–246.

Clauzon, G., 1980a. Le canyon messinien de la Durance (Provence, France): une preuve paléogéographique du basin profond de dessiccation. Palaeogeography, Palaeoclimatology, Palaeoecology 29, 15–40.

Clauzon, G., 1980b. Révision de l'interprétation géodynamique du passage Miocène–Pliocène dans le bassin de Vera (Espagne méridionale): les coupes d'Antas et de Cuevas del Almanzora. Rivista Italiana di Paleontologia 86 (1), 203–214.

Clauzon, G., 1982. Le canyon messinien du Rhône: une preuve décisive du "desiccated deep-basin model" (Hsü, Cita et Ryan, 1973). Bulletin de la Société Géologique de France Série 7 24 (3), 597–610.

Clauzon, G., 1990. Restitution de l'évolution géodynamique néogène du bassin du Roussillon et de l'unité adjacente des Corbières d'après les données écostratigraphiques et paléogéographiques. Paléobiologie Continentale 17, 125–155.

Clauzon, G., 1999. L'impact des variations eustatiques du basin de Méditerranée occidentale sur l'orogène alpin depuis 20 Ma. Etudes de Géographie Physique 28, 1–8.

Clauzon, G., Suc, J.-P., Aguilar, J.-P., Ambert, P., Cappetta, H., Cravatte, J., Drivaliari, A., Doménech, R., Dubar, M., Leroy, S., Martinell, J., Michaux, J., Roiron, P., Rubino, J.-L., Savoye, B., Vernet, J.-L., 1990. Pliocene geodynamic and climatic evolutions in the French Mediterranean region. Paleontologia i Evolucio. Memòria Especial 2, 132–186.

Clauzon, G., Suc, J.-P., Gautier, F., Berger, A., Loutre, M.-F., 1996. Alternate interpretation of the Messinian salinity crisis: controversy resolved? Geology 24, 363–366.

Clauzon, G., Suc, J.-P., Popescu, S.-M., Mărunţeanu, M., Rubino, J.-L., Marinescu, F., Melinte, M.C., 2005. Influence of the Mediterranean sea-level changes over the Dacic Basin (Eastern Paratethys) in the Late Neogene. The Mediterranean Lago Mare facies deciphered. Basin Research 17, 437–462.

Clauzon, G., Suc, J.-P., Popescu, S.-M., Melinte-Dobrinescu, M.C., Quillévéré, F., Warny, S.A., Fauquette, S., Armijo, R., Meyer, B., Rubino, J.-L., Lericolais, G., Gillet, H., Çağatay, M.N., Ucarkus, G., Escarguel, G., Jouannic, G., Dalesme, F., 2008. Chronology of the Messinian events and paleogeography of the Mediterranean region *s.l.* CIESM Workshop Monographs 33, 31–37.

Cornée, J.-J., Ferrandini, M., Saint Martin, J.-P., Münch, Ph., Moullade, M., Ribaud-Laurenti, A., Roger, S., Saint Martin, S., Ferrandini, J., 2006. The late Messinian erosional surface and the subsequent reflooding in the Mediterranean: new insights from the Melilla–Nador basin (Morocco). Palaeogeography, Palaeoclimatology, Palaeoecology 230 (1–2), 129–154.

Cour, P., 1974. Nouvelles techniques de détection des flux et de retombées polliniques: étude de la sédimentation des pollens et des spores à la surface du sol. Pollen et Spores 16 (1), 103–141.

Delrieu, B., Rouchy, J.M., Foucault, A., 1993. La surface d'érosion finimessinienne en Crète centrale (Grèce) et sur le pourtour méditerranéen: Rapport avec la crise de salinité méditerranéenne. Comptes-Rendus de l'Académie des Sciences de Paris Série 2 318, 1103–1109.

El Euch-El Koundi, N., Ferry, S., Suc, J.-P., Clauzon, G., Melinte-Dobrinescu, M.C., Gorini, C., Safra, A., El Koundi, M., Zargouni, F., 2009. Messinian deposits and erosion in

northern Tunisia: inferences on the Sicily Strait during the Messinian Salinity Crisis. Terra Nova 21, 41–48.
Ellegaard, M., 2000. Variations in dinoflagellate cyst morphology under conditions of changing salinity during the last 2000 years in the Limfjord, Denmark. Review of Palaeobotany and Palynology 109, 65–81.
Esu, D., 2007. Latest Messinian "Lago-Mare" Lymnocardiinae from Italy: close relations with the Pontian fauna from the Dacic Basin. Geobios 40, 291–302.
Faranda, C., Gliozzi, E., Ligios, S., 2007. Late Miocene brackish Loxoconchidae (Crustacea, Ostracoda) from Italy. Geobios 40, 303–324.
Fauquette, S., Guiot, J., Suc, J.-P., 1998. A method for climatic reconstruction of the Mediterranean Pliocene using pollen data. Palaeogeography, Palaeoclimatology, Palaeoecology 144, 183–201.
Fauquette, S., Clauzon, G., Suc, J.-P., Zheng, Z., 1999. A new approach for paleoaltitude estimates based on pollen records: example of the Mercantour Massif (south-eastern France) at the earliest Pliocene. Earth and Planetary Science Letters 170, 35–47.
Gautier, F., Clauzon, G., Suc, J.-P., Cravatte, J., Violanti, D., 1994. Age et durée de la crise de salinité messinienne. Comptes-Rendus de l'Académie des Sciences de Paris Série 2 318, 1103–1109.
Gillet, S., Gramann, F., Steffens, P., 1978. Neue biostratigraphische Ergebnisse aus dem brackischen Neogen an Dardanellen und Marmara–Meer (Türkei). Newsletters of Stratigraphy 7, 53–64.
Gillet, H., Lericolais, G., Réhault, J.-P., 2007. Messinian event in the black sea: evidence of a Messinian erosional surface. Marine Geology 244, 142–165.
Gliozzi, E., Ceci, M.A., Grossi, F., Ligios, S., 2007. Paratethyan Ostracods immigrants in Italy during the Late Miocene. Geobios 40, 325–337.
Görür, L., Çağatay, M.N., Sakınç, M., Sumengen, M., Senturk, K., Yaltırak, C., Tchapalyga, A., 1997. Origin of the Sea of Marmara deduced from Neogene to Quaternary paleogeographic evolution of its frame. International Geological Review 39, 342–352.
Görür, L., Çağatay, M.N., Sakınç, M., Tchapalyga, A., Akkök, R., Natalin, B., 2000. Neogene Paratethyan succession in Turkey and its implications for paleogeographic evolution of the Eastern Paratethys. In: Bozkurt, E., Winchester, J.A., Piper, J.A.D. (Eds.), Tectonics and Magmatism in Turkey and Surrounding Area. Geological Society of London Special Publication, vol. 173, pp. 251–269.
Guennoc, P., Gorini, C., Mauffret, A., 2000. Histoire géologique du Golfe du Lion et cartographie du rift oligo-aquitanien et de la surface messinienne. Géologie de la France 3, 67–97.
Hallett, R.I., 1999. Consequences of environmental change on the growth and morphology of *Lingulodinium polyedrum* (Dinophyceae) in culture. Thesis, Westminster Univ. London, 109 pp.
Hsü, K.J., Cita, M.B., Ryan, W.B.F., 1973. The origin of the Mediterranean evaporites. Initial Reports of the Deep Sea Drilling Project 42, 1203–1231.
Kokinos, J.P., Anderson, D.M., 1995. Morphological development of resting cysts in cultures of the marine dinoflagellate *Lingulodinium polyedrum* (= *L. machaerophorum*). Palynology 19, 143–166.
Lofi, J., Rabineau, M., Gorini, C., Berné, S., Clauzon, G., De Clarens, P., Dos Reis, T., Mountain, G.S., Ryan, W.B.F., Steckler, M., Fouchet, C., 2003. Plio-Quaternary prograding clinoform wedges of the Western Gulf of Lions continental margin (NW Mediterranean) after the Messinian Salinity Crisis. Marine Geology 198, 289–317.
Lofi, J., Gorini, C., Berné, S., Clauzon, G., Dos Reis, A.T., Ryan, W.B.F., Steckler, M.S., 2005. Erosional processes and paleo-environmental changes in the western gulf of Lion (SW France) during the Messinian salinity crisis. Marine Geology 217, 1–30.
Lourens, L.J., Hilgen, F.J., Laskar, J., Shackleton, N.J., Wilson, D., 2004. The Neogene period. In: Gradstein, F.M., Ogg, J.G., Smith, A.G. (Eds.), A geological Time Scale 2004. Cambridge University Press, Cambridge, pp. 409–440.
Maillard, A., Mauffret, A., 2006. Relationship between erosion surfaces and Late Miocene Salinity Crisis deposits in the Valencia Basin (northwestern Mediterranean): evidence for an early sea-level fall. Terra Nova 18, 321–329.
Marinescu, F., 1992. Les bioprovinces de la Paratéthys et leurs relations. Paleontologia i Evolució 24–25, 445–453.
Marret, F., Zonneveld, K.A.F., 2003. Atlas of modern organic-walled dinoflagellate cyst distribution. Review of Palaeobotany and Palynology 125, 1–200.
Martini, E., 1971. Standard Tertiary and Quaternary calcareous nannoplankton zonation. In: Farinacci, A. (Ed.), Proceedings of the 2nd International Conference on Planktonic Microfossils, Roma 1970, vol. 2. editura Tecnoscienza, Rome, pp. 739–785.
Mărunţeanu, M., Papaianopol, I., 1995. The connection between the Dacic and Mediterranean Basins based on calcareous nannoplankton assemblages. Romanian Journal of Stratigraphy 76, 169–170.
Melinte, M.C., 2006. Cretaceous–Cenozoic paleobiogeography of the southern Romanian Black Sea onshore and offshore areas. Geo-Eco-Marina 12, 79–90.
Ozenda, P., 1989. Le déplacement vertical des étages de vegetation en fonction de la latitude: un modèle simple et ses limites. Bulletin de la Société Géologique de France Série 8 5 (83), 535–540.
Perch-Nielsen, K., 1985. Cenozoic calcareous nannofossils. In: Bolli, H.M., Saunders, J.B., Perch-Nielsen, K. (Eds.), Plankton Stratigraphy. Cambridge University Press, Cambridge, pp. 427–554.
Poisson, A., Wernli, R., Sağular, E.K., Temiz, H., 2003. New data concerning the age of the Aksu Thrust in the south of the Aksu valley, Isparta Angle (SW Turkey): consequences for the Antalya Basin and the Eastern Mediterranean. Geological Journal 38, 311–327.
Popescu, S.-M., 2006. Upper Miocene and Lower Pliocene environments in the southwestern Black Sea region from high-resolution palynology of DSDP site 380A (Leg 42B). Palaeogeography, Palaeoclimatology, Palaeoecology 238, 64–77.
Popescu, S.-M., Suc, J.-P., Melinte, M., Clauzon, G., Quillévéré, F., Sütő-Szentai, M., 2007. Earliest Zanclean age for the Colombacci and uppermost Di Tetto formations of the "latest Messinian" northern Apennines: new palaeoenvironmental data from the Maccarone section (Marche Province, Italy). Geobios 40 (3), 359–373.
Popescu, S.-M., Dalesme, F., Jouannic, G., Escarguel, G., Head, M.J., Melinte-Dobrinescu, M.C., Sütő-Szentai, M., Bakrac, K., Clauzon, G., Suc, J.-P., 2009. *Galeacysta etrusca* complex, dinoflagellate cyst marker of Paratethyan influxes into the Mediterranean Sea before and after the peak of the Messinian Salinity Crisis. Palynology 33 (1).
Popov, S.V., Shcherba, I.G., Ilyina, L.B., Nevesskaya, L.A., Paramonova, N.P., Khondkarian, S.O., Magyar, I., 2006. Late Miocene to Pliocene palaeogeography of the Paratethys and its relation to the Mediterranean. Palaeogeography, Palaeoclimatology, Palaeoecology 238 (1–4), 91–106.
Quézel, P., 1998. Cèdres et cédraies du pourtour méditerranéen: signification bioclmatique et phytogéographique. Forêt méditerranéenne 19 (3), 243–260.
Quézel, P., Médail, F., 2003. Ecologie et biogéographie des forets du bassin méditerranéen. Elsevier, Paris. 570 pp.
Raffi, I., Backman, J., Fornaciari, E., Pälike, H., Rio, D., Lourens, L.J., Hilgen, F.J., 2006. A review of calcareous nannofossil astrobiochronology encompassing the past 25 million years. Quaternary Science Reviews 25, 3113–3137.
Raffi, I., Mozzato, C., Fornaciari, E., Hilgen, F.J., Rio, D., 2003. Late Miocene calcareous nannofossil biostratigraphy and astrobiochronology for the Mediterranean region. Micropaleontology 49 (1), 1–26.
Rögl, F., 1998. Palaeogeographic considerations for Mediterranean and Paratethys seaways (Oligocene to Miocene). Annales des Naturhistorichen Museums in Wien 99 (A), 279–310.
Rögl, F., Steininger, F.F., 1983. Vom Zerfall der Tethys zu Mediterran uns paratethys. Die neogene Paläogeographie und Palinspastik des zirkum-mediterranean Raumes. Annales des Naturhistorischen Museums in Wien 85 (A), 135–163.
Rouchy, J.-M., Suc, J.-P., Ferrandini, J., Ferrandini, M., 2006. The Messinian Salinity Crisis revisited. Sedimentary Geology 188–189, 1–8.
Sage, F., Von Gronefeld, G., Déverchère, J., Gaullier, V., Maillard, A., Gorini, C., 2005. Seismic evidence for Messinian detrital deposits at the western Sardinia margin, northwestern Mediterranean. Marine and Petroleum Geology 22, 757–773.
Sakınç, M., Yaltırak, C., 2005. Messinian crisis: what happened around the northeastern Aegean? Marine Geology 221, 423–436.
Sakınç, M., Yaltırak, C., Oktay, F.Y., 1999. Palaeogeographical evolution of the Thrace Neogene Basin and the Tethys–Paratethys relations at northwestern Turkey (Thrace). Palaeogeography, Palaeoclimatology, Palaeoecology 153, 17–40.
Seneš, J., 1973. Correlation hypotheses of the Neogene Tethys and Paratethys. Giornale di Geologia 39, 271–286.
Snel, E., Mărunţeanu, M., Meulenkamp, J.E., 2006. Calcareous nannofossil biostratigraphy and magnetostratigraphy of the Upper Miocene and Lower Pliocene of the Northern Aegean (Orphanic Gulf-Strimon Basin areas), Greece. Palaeogeography, Palaeoclimatology, Palaeoecology 238, 107–124.
Sorrel, P., Popescu, S.-M., Head, M.J., Suc, J.-P., Klotz, S., Oberhänsli, H., 2006. Hydrographic development of the Aral Sea during the last 2000 years based on a quantitative analysis of dinoflagellate cysts. Palaeogeography, Palaeoclimatology, Palaeoecology 234, 304–327.
Sprovieri, M., Sacchi, M., Rohling, E.J., 2003. Climatically influenced interactions between the Mediterranean and the Paratethys during the Tortonian. Paleoceanography 18 (2), 12–1–12-10.
Stoica, M., Lazăr, I., Vasiliev, I., Krijgsman, W., 2007. Mollusc assemblages of the Pontian and Dacian deposits from the Topolog–Arges area (southern Carpathian foredeep — Romania). Geobios 40, 391–405.
Suc, J.-P., Rouchy, J.M., Ferrandini, M., Ferrandini, J., 2007. Editorial. The Messinian Salinity Crisis revisited. Geobios 40 (3), 231–232.
Taner, G., 1979. Die Molluskenfauna der Neogenen Formationen der Halbinsel - Gelibolu. Annales Géologiques des Pays Helléniques out of Series, 3, 1189–1194.
Ternek, Z., 1964. Geological map of Turkey at 1/500.000: Istanbul. Maden Tetkik ve Arama Enstitüsü Hazirlamiş ve Yayinlamiştir, Ankara.
Türkecan, A., Yurtsever, A., 2002. Geological map of Turkey at 1/500.000: Istanbul. Maden Tetkik ve Arama Genel Müdürlüğü, Ankara.
Van Couvering, J.A., Castradori, D., Cita, M.B., Hilgen, F.J., Rio, D., 2000. The base of the Zanclean Stage and of the Pliocene Series. Episodes 23 (3), 179–187.
Wade, B.S., Bown, P.R., 2006. Calcareous nannofossils in extreme environments: the Messinian Salinity Crisis, Polemi Basin, Cyprus. Palaeogeography, Palaeoclimatology, Palaeoecology 233, 271–286.
Yaltırak, C., Sakınç, M., Oktay, F.Y., 2000. Westward propagation of North Anatolian fault into the northern Aegean: timing and kinematics: comment. Geology 28, 187–188.
Young, J.R., 1998. Chapter 9: Neogene. In: Bown, P.R. (Ed.), Calcareous Nannofossils Biostratigraphy. British Micropaleontological Society Publications Series. Kluwer Academic Press, Dordrecht, pp. 225–265.